Accident Analysis and Prevention 157 (2021) 106170

Contents lists available at ScienceDirect

Accident Analysis and Prevention

journal homepage: www.elsevier.com/locate/aap

The influence of car passengers' sitting postures in intersection crashes

Alexandros Leledakis [a,b,*], Jonas Östh [a,b], Johan Davidsson [a], Lotta Jakobsson [a,b]

[a] Chalmers University of Technology, SE-412 96, Gothenburg, Sweden
[b] Volvo Car Corporation, SE-405 31, Gothenburg, Sweden

ARTICLE INFO

Keywords:
Finite element
Frontal impact
Human body model
Occupant kinematics
Occupant sitting postures
Real-world safety
Side impact
Vehicle safety assessment

ABSTRACT

Car passengers are frequently sitting in non-nominal postures and are able to perform a wide range of activities since they are not limited by tasks related to vehicle control, contrary to drivers. The anticipated introduction of Autonomous Driven vehicles could allow "drivers" to adopt similar postures and being involved in the same activities as passengers, allowing them a similar set of non-nominal postures. Therefore, the need to investigate the effects of non-nominal occupant sitting postures during relevant car crash events is becoming increasingly important.

This study aims to investigate the effect of different postures of passengers in the front seat of a car on kinematic and kinetic responses during intersection crashes. A Human Body Model (HBM) was positioned in a numerical model of the front passenger seat of a midsize Sports Utility Vehicle (SUV) in a total of 35 postures, including variations to the lower and upper extremities, torso, and head postures. Three crash configurations, representative of predicted urban intersection crashes, were assessed in a simulation study; two side impacts, a near-side and a far-side, respectively, and a frontal impact. The occupant kinematics and internal loads were analyzed, and any deviation between the nominal and altered posture responses were quantified using cross-correlation of signals to highlight the most notable variations.

Posture changes to the lower extremities had the largest overall influence on the lower extremities, pelvis, and whole-body responses for all crash configurations. In the frontal impact, crossing the legs allowed for the highest pelvis excursions and rotations, which affected the whole-body response the most. In the two side-impacts, leaning the torso in the coronal plane affected the torso and head kinematics by changing the interaction with the vehicle's interior. Additionally, in far-side impacts supporting the upper extremity on the center console resulted in increased torso excursions. Moreover, the response of the upper extremities was consistently sensitive to posture variations of all body regions.

1. Introduction

Car passengers can adopt a wide range of postures while traveling in a car. A volunteer-based survey of preferred postures, conducted by Zhang et al. (2004), indicates that front seat passengers were seated in the nominal posture (upright, centered in the seat, looking in the direction of travel with feet on the footrest) for approximately 45 % of a daily trip. The anticipated introduction of Autonomous Driven (AD) vehicles could potentially influence the seating position preferences, and occupant activity patterns (Koppel et al., 2019; Nie et al., 2020) and broaden the selection of posture and activity options for passengers and "drivers" of future AD vehicles. Therefore, the need to evaluate the protection of future drivers and passengers of AD vehicles traveling seated in postures deviating from the nominal when involved in car crashes, is growing.

A number of studies have highlighted the influence of the occupant's pre-impact posture on injury risk in vehicle crashes. Bose et al. (2010) used a multibody Human Body Model (HBM) to investigate the influence of occupant characteristics such as stature, mass, posture, and muscle bracing level to injury risk in frontal crashes and identified that the occupant's posture generated the largest effect on the outcome. Furthermore, a sensitivity analysis carried out by Hwang et al. (2016) using an HBM showed that in side-impact conditions, the body posture was an important aspect for predicting occupant impact responses. Those findings have been reinforced during the model validation work conducted by Park et al. (2016), in which it was found that considering the initial posture was an influential parameter for predicting the shoulder kinematics during lateral impacts. Matching the initial posture

* Corresponding author at: Chalmers University of Technology, Hörselgången 4, SAGA Building, Floor 4, SE-417 56, Gothenburg, Sweden.
E-mail address: alexandros.leledakis@chalmers.se (A. Leledakis).

https://doi.org/10.1016/j.aap.2021.106170
Received 8 February 2021; Received in revised form 7 April 2021; Accepted 2 May 2021

of the HBM with the initial posture of the subject, altered the orientation of the clavicle relative to the impact direction and led to increased shoulder rotation, improving the prediction of the peak shoulder deflection by 24 %.

Interaction with the restraint systems can also be sensitive to occupant postures, as shown by Gierczycka and Cronin (2017), who showed that the injury risk was more sensitive to the pre-crash arm position compared with the selection of restraint system combinations. Furthermore, Nie et al. (2017) investigated knee airbag designs for frontal and oblique impacts. Tibia bending moment and axial load were increased for occupants with a smaller gap between the knee and the instrument panel, indicating that the relative position of the lower extremities can be an important aspect of occupant crash response.

The effect of spinal posture on predicted injury risk in vehicle crashes has attracted considerable interest from researchers. Predicted reaction forces and rib strains can be greatly affected by spinal posture both in frontal (Poulard et al., 2015b) and side impacts (Poulard et al., 2014). Modifying the spinal posture created comparable variability in the impact response, as observed in Post-Mortem Human Subject (PMHS) experiments with different anthropometries (Poulard et al., 2014). Additionally, Izumiyama et al. (2018) analyzed individual differences in skeletal alignment using HBMs. X-ray images from 75 individuals were clustered in two groups based on their lumbar spinal alignment; S-shaped or kyphotic. Multiple HBMs were morphed based on that analysis. Their pelvic motion in frontal crashes was affected by the lumbar spinal alignment with the pelvis tilting rearward, showing tendencies for higher excursions and rotations.

The kinematic and kinetic responses may be suitable as injury indicators. Gabler et al. (2016) published a comparative study, assessing kinematic brain injury metrics and identified rotational head kinematics as the most important kinematic metrics for brain injury risk prediction by correlating it with brain strain. Brain Injury Criterion (BrIC), which is using the maximum magnitudes of the head angular velocity components, was among the best correlating criteria. Furthermore, Logistic regression was applied to data from the thoracic and lumbar vertebral columns of three PMHSs by Yoganandan et al. (2013) identifying 3.4 kN as the force level corresponding to 50 % probability of spinal injury.

Even though previous studies have investigated the influence of occupant postures, such as 'leaning torso' and modified upper extremity postures, there is a need to further understand which postures influence the occupant injury risk the most. Additionally, more insight into how the posture of one body region affects the in-crash response of the whole body or another body region is also of interest. The objective of this study is to investigate the effect of front-seat passengers' sitting postures on kinematic and kinetic responses, by varying the posture of the lower extremities, torso, upper extremities, and the head, followed by systematic analysis of the responses. Crash configurations representative of predicted real-world urban intersection crashes, extending beyond the scope of standardized testing, have been applied.

2. Methods

A simulation series using a mid-sized male HBM in the front passenger seat of a mid-sized SUV was performed, including posture variations of the lower extremities, torso, upper extremities, and the head. In total, 35 Occupant Sitting Postures (OSP) were simulated in three different crash configurations, representative of intersection crashes.

2.1. Models

A car passenger was modeled using the SAFER HBM v9 positioned in the front right seat of a mid-sized SUV passenger compartment model, Fig. 1, equipped with the current state-of-the-art restraint systems.

The passenger compartment sled was modeled using a rigid body-in-white with a deformable interior with approximately 2.35 million Finite Elements (FE). The occupant was modeled using the SAFER HBM v9.0.1

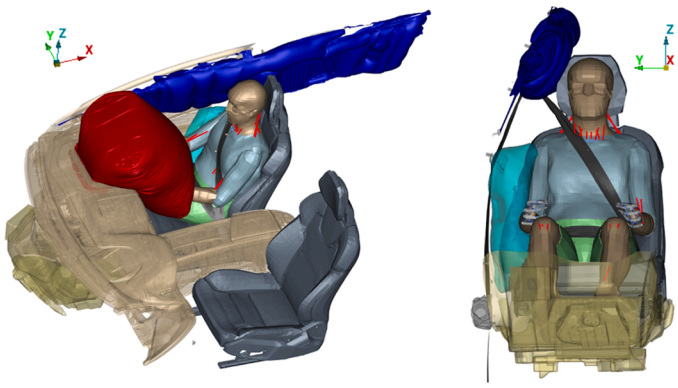

Fig. 1. The passenger compartment FE model with the SAFER HBM positioned in the nominal occupant sitting posture and deployed airbags (frontal in red, inflatable curtain in blue, and torso in cyan).

(Östh et al., 2020), representing a 50th percentile male, with a stature of 175 cm and weight of 77 kg, in accordance with Schneider et al. (1983). The biofidelity of the SAFER HBM v9, has been evaluated in frontal, near- and far- side impacts, and been employed for detailed accident reconstructions of diverse real-world crashes (Pipkorn et al., 2019). In a frontal sled impact, the HBM showed good biofidelity for the upper-body kinematics (Iraeus and Pipkorn, 2019), and even for reclined (50°) occupants there was a good correlation in the excursions of the Head, T1, T8, T11, L1, L3 and pelvis between the model response and sled tests with PMHSs (Mroz et al., 2020). Good cross-correlation was also found for the lateral torso velocities between the model and PMHSs data in a near-side sled impact (Larsson et al., 2019). Additionally, the model was considered adequate for the evaluation of head excursions in far-side impacts (Pipkorn et al., 2018).

The seat was set at mid-height, low-tilt, mid-fore/aft position, and the seat-back angle was set to 25° for an upright, and 30° for a semi-reclined, position. The occupant was restrained using a three-point pyrotechnically-pretensioned load-limited seatbelt, a frontal passenger airbag deploying from the dashboard, and for the side impacts, a seat-mounted torso airbag and an inflatable curtain, Fig. 1. The restraint system's activation timing is presented in Table A.1 (Appendix A). Validation of the passenger compartment model was performed by simulating a FE Hybrid III Anthropomorphic Test Device (ATD) and comparing it with a full-scale physical crash test. The passenger compartment model was considered a good representation of the real vehicle (Appendix B).

A right-handed coordinate system was used, defined with X rearward, Z upward, and Y toward the right side of the vehicle, Fig. 1. The explicit FE solver LS-DYNA MPP s R9.3.0 (LSTC, Livermore, CA, USA) was used for all simulations.

2.2. Crash configurations

Three crash configurations, representative of a number of diverse potential future intersection crashes (Leledakis et al., 2021), were selected for this study. A Near-Side side-impact to the front right corner, a Far-Side side-impact to the front left corner, and a Frontal impact with approximately 50 % overlap from the left (Fig. 2), were simulated. The selected crash configurations were derived from real-world crashes and are representative of the crash configurations expected to be seen in urban intersections after the introduction of crash-avoidance countermeasures with wide field-of-view sensors.

Crash pulses were generated by simulating car to car (car-car) impacts with a mid-sized station wagon FE car model, using the simulation environment described by Wågström et al. (2013), which has been previously validated against physical crash tests. The resulting crash pulses can be described as relatively low-severity crashes. The z-rotation

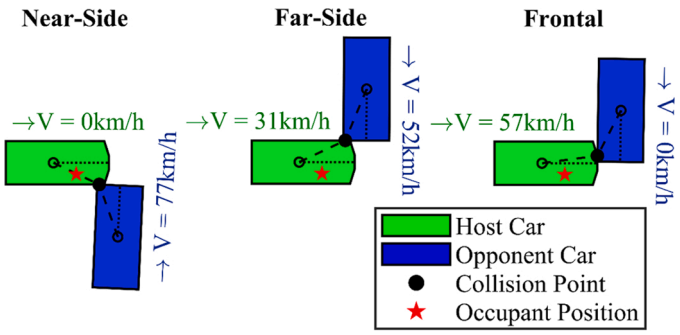

Fig. 2. The three crash configurations from left to right, two side impacts; a Near-Side, and a Far-Side, and a Frontal impact can be seen.

of the Near-Side impact reached up to 5.8 rad/s, and the peak lateral acceleration was 26.8 g in the Far-Side impact. In the Frontal crash, the peak resultant acceleration was 22.9 g, and the resultant ΔV was 5.8 m/s. The in-crash vehicle motions are illustrated in Appendix C – Fig. C.2, and the crash configurations, along with the severity measures, are presented in Appendix C – Table C.1.

For the occupant in-crash simulations, the motion from the car-car impacts was applied to the compartment model by prescribed rigid body six-degrees-of-freedom translational and rotational velocities.

2.3. Occupant positioning

The HBM was positioned in the target OSPs by pre-simulation using the marionette method (Poulard et al., 2015a). One-dimensional elements were used to pull selected body landmarks to the desired position, consequently moving the HBM into position. The positioning was performed in multiple stages when the target posture required complex motions to be achieved. During the HBM positioning process, the posture of the extremities, torso, and head was controlled. However, the orientation of the pelvis and the spinal alignment was determined by the biomechanical properties of the HBM. The HBM stresses generated through the positioning process were not re-initialized for the impact simulations. After positioning the HBM, the belt was routed to the shortest path, removing the slack, using the belt routing algorithm of the Primer v16 (Oasys Ltd, Sollihull, United Kingdom) software.

2.4. Passenger sitting postures

In total, 35 different OSPs were included in the study. The nominal posture was set up similarly to the procedure specified for ATD front passengers (European New Car Assessment Programme (Euro NCAP, 2020a). The feet rested on the footrest with extended knees, and the distance between the knees and the dashboard was approximately 30 mm. The torso was in contact with the backrest and centered in the seat, the arms were adjacent to the torso and the hands rested on the side of the thighs. Body region postures (Fig. 3) deviating from the nominal posture, were then introduced; seven for the lower extremities, eight for the torso, four for the upper extremities, and three for the head. The lower and upper extremity postures were specified relative to the passenger compartment's geometrical constraints, such as the floor-pan, the center console, and the door panel. The different body region postures are described in Sections 2.4.1 – 2.4.4.

The OSPs were generated by incrementally combining different body region postures, starting from the lower extremities and torso, and concluding with the upper extremities and the head postures. The complete posture matrix and a more detailed depiction of the postures can be seen in Appendix D.

2.4.1. Lower extremities

The occupant's lower extremities were positioned in the extended knees (nominal), flexed knees, crossed legs, and locked ankles postures. The lower extremities were positioned relative to the geometrical constraints of the vehicle interior, by adjusting the knee and ankle angles so that the feet surfaces were in contact and parallel with the footrest. The resulting postures are further described in the paragraphs below.

The femur and tibia were parallel with the XZ-plane in the extended knees posture, which was the nominal posture. The occupant's feet rested on the passenger footrest, and the knee flexion angles were approximately 105°.

For the flexed knees posture, the feet have been moved rearward, so that they were parallel with the vehicle floor and as close to the seat as possible. The thighs have been lifted as a consequence of the motion and the resulting knee flexion angle was approximately 65°.

Combining the extended knees and the flexed knees posture generated the one knee flexed posture, where either the right or the left foot was moved rearward, targeting 65° for the knee flexion angle.

Two postures featuring crossed legs were generated, with either the left or the right leg placed over the opposite knee. Three stages were used to achieve the desired posture. First, the thigh was lifted, then rotated medially (≈20°–30°), and finally, the knee was flexed so that the tibia was almost parallel to the z-axis. The target posture was derived through the geometric constraints of the vehicle interior and the manipulated knee flexion angle settled at approximately 65°–75°. The distance between the knee and the dashboard was measured at 112 mm and 140 mm when the right and the left leg were crossed over the opposite knee, respectively. Additionally, crossing the legs resulted in altered lap belt fit, with the lap belt positioned higher relative to the ASIS on the pelvis, especially on the side of the leg that was over due to altered shape of the soft tissue in the region. The lap belt fit for all lower extremity postures is displayed in Appendix E.

Positioning the HBM to match a person in locked ankles (with the right leg over the opposite ankle) posture was performed in two steps; Starting from the nominal posture, the (right) knee was first extended

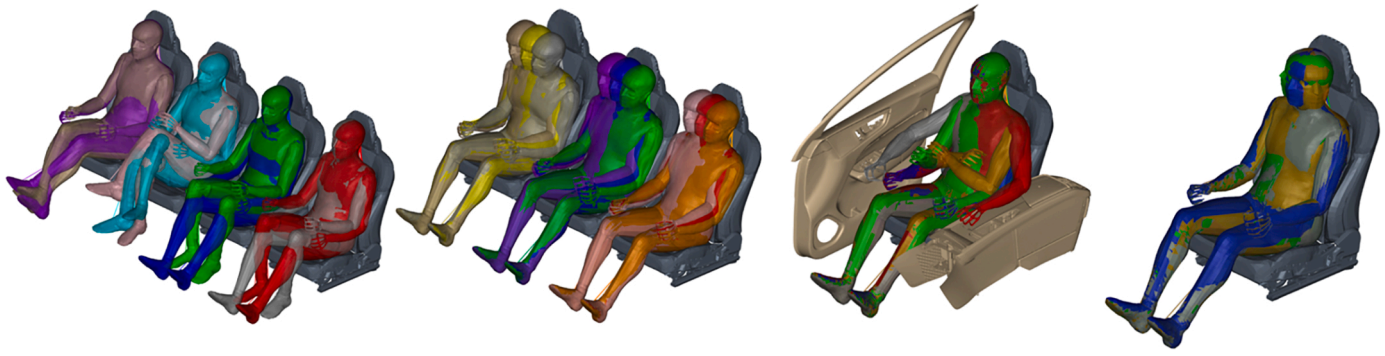

Fig. 3. Overview of the body region postures used in this study. From left to right, the lower extremities, torso (nominal / semi-reclined / forward-leaning), upper extremities, and head torso variations can be seen.

while the opposite hip-joint was rotated 10° medially, and then the (right) hip-joint was rotated (≈10°) medially and the knee flexed until the leg was over the opposite ankle. One posture with the left and one with the right leg over the opposite ankle were generated and the leg that was crossed over was 4 mm away from the dashboard. The lower extremities are one of the main load paths during frontal impacts; therefore, variations of their posture were of interest for this study. As observed in a recent study by Bohman et al. (2020b), the lower extremities represented the body region with the most variations in posture in a stationary vehicle experiment. In a naturalistic study by Reed et al. (2020a), the nominal posture (extended knees) was found to be the most frequent lower extremity posture, followed by flexed knees (40 %) and crossed legs (6 %). It should also be noted that "crossed legs" in the literature can frequently refer to either locked ankles or "crossed at the knee".

2.4.2. Torso

Variations in the torso postures were considered in the sagittal and coronal planes for this study. Three postures were considered for the sagittal plane. The nominal posture was with the occupant fully seated in a seat at 25° seat-back angle. The occupant was also positioned in a semi-reclined posture with the seat-back angle adjusted to 30°, and leaning forward with reduced contact to the seat-back (at the nominal 25° seat-back angle). In the leaning forward posture, the head's Center of Gravity (CoG) is translated 108 mm longitudinally, which is conservative compared to measurements (mean translation ≈300 mm) from occupants who were asked to "reach as far as possible forward" (Reed et al., 2021). However, the head position in the leaning forward posture is comparable to the position during a braking event (Ólafsdóttir et al., 2013). The resulting torso y-angle (in the XZ-plane), measured from the sacrum's posterior surface to the T8 spinous process in the sagittal plane (Appendix D), was 27°, 34°, and 19°, in these postures, respectively. Variations on the shoulder belt fit were observed when the occupant leaned forward or backward. More specifically, the shoulder belt was positioned higher on the sternum and more proximal on the clavicle when the occupant was semi-reclined and lower on the sternum and more distal on the clavicle when the occupant was leaning forward (Appendix E).

Furthermore, three posture variations were generated in the coronal plane for every posture of the torso in the sagittal plane. In the nominal posture, the centerline of the occupant aligned with the centerline of the seat. Additional postures, in which the occupant tilted 6.4° inboard (left) and -6.4°outboard (right), were also generated. The torso tilt (torso x-angle) was measured from the posterior surface of the sacrum to the T8 vertebral body (Appendix D). The amount of torso tilt was based on data from everyday traffic (Bohman et al., 2020a). Specifically, for the leaning inboard posture, the leaning torso resulted in approximately 95 mm of lateral translation for the Head CoG, which is within one standard deviation of the measurements of Reed et al. (2021). Leaning in the coronal plane altered mainly the shoulder belt fit, with minor variation in the lap belt due to the pelvis rotation in the coronal plane. Leaning inboard positioned the belt lower on the sternum and more distal on the clavicle. On the contrary, leaning outboards moved the belt higher on the sternum and more proximal on the clavicle relative to the nominal posture. More details of the belt fit can be found in Appendix E.

Variations of the torso posture can be introduced based on occupant preference or chosen activity. During naturalistic driving, the occupant's torso was found in the nominal posture for approximately 85 % of the time (Reed et al., 2020b), while tilting inboard or outboard accounted for approximately 7 % of the travel duration, and 10 % of the time, the occupant was leaning forward. In a driving study (Bohman et al., 2020a), while the vehicle was turning, the lateral torso position was significantly different to the torso position prior to the turn, with the average lateral movement ranging between 25 mm and 45 mm. Besides normal driving, occupant movement can be induced by acceleration due to driving maneuvers, such as braking (Östh et al., 2013) or changing lanes (Ghaffari et al., 2018), and consequently affects the pre-impact posture.

2.4.3. Upper extremities

For the nominal upper extremity posture, the occupant's upper arms were positioned adjacent to the torso and the hands were placed over the occupant's knees. The nominal upper extremity posture, along with selected additional upper extremity postures, were generated for all torso postures.

Postures with the occupant's upper extremities supported on the vehicle's armrests were generated. The occupant's right elbow was positioned in contact with the door armrest for all torso postures when the occupant was not leaning inboard. Additionally, the occupant's left elbow was positioned in contact with the center console armrest for all torso postures when the occupant was not leaning outboard.

Two additional postures were assessed when the occupant was not leaning forward, inboard, or outboard. The occupant was positioned with arms crossed over the chest by placing the occupant's left forearm over the right in the height of the xiphoid process. Moreover, the posture of holding a phone was replicated by rotating the occupant's right arm medially to the height of the xiphoid process. The depiction of the postures is available in Appendix D (Fig. D.3a–h).

A photographic analysis (Bingley et al., 2005) suggested that 46 % of the front row passengers kept both hands on their lap, while crossed arms was the second most frequently observed posture at 4 %. Data from Reed et al. (2020b) suggest that the upper extremity postures were more diverse, with frequent contact with the torso (36 %–40 %), lower extremities (19 %–34 %), and armrest (7 %–17 %). Additionally, passengers spent approximately 26 % of their time on their phones (Reed et al., 2020b).

2.4.4. Head

Besides the nominal head posture, set with the head facing the vehicle's traveling direction, three more head postures were generated. The head was turned approximately 60° left and 55° right, representing a look towards the driver – or Left-Hand Side (LHS) occupant – and outboard, respectively. Additionally, the head was turned approximately 80° right, representing taking a look over the shoulder. The initial head orientation for every target head posture was derived from naturalistic data of drivers (Fice et al., 2018) by mirroring the Frankfort plane on the XZ-plane to match a LHS occupant, and can be found in Appendix D – Table D.5.

Occupants and drivers can be expected to look toward other occupants (during discussions, etc.) and/or toward the environment. According to Fice et al. (2018), drivers spend a larger proportion of time with their heads in non-neutral postures when the vehicle is stationary (17 %) compared to moving (8 %). Similarly, in a naturalistic study, front passengers had their heads rotated left in 14 % or right in 19 % of the analyzed frames (Reed et al., 2020a).

2.5. Analysis

The kinematic response was analyzed by tracking the 3-dimensional excursions of anatomical landmarks, the pelvic angle (Izumiyama et al., 2018), torso angle, and the head Frankfurt plane orientation. The torso angle was defined on the XZ and YZ plane using the sacrum and T8 vertebra, while the left and right acromion were used to calculate torso rotation around the z-axis. As part of the kinematic response, the head Center of Gravity (CoG) and sternum (x,y,z, and resultant) velocity, relative to the vehicle, was also tracked. In addition, loads (x-, y-, z-, and resultant forces and moments) at cross-sections of the HBM were extracted and compared. The landmarks excursions, angles, velocities, and cross-section loads used in the analysis can be found in Table 1 and are illustrated in Appendix F.

Cross-correlation was performed, using CORA (Gehre and Stahlschmidt, 2011), to systematically quantify the extent of the change in

Table 1
Anatomical landmarks excursion (exc.) (black), angles (blue), velocities (red), and cross-section loads (green).

Lower extremities - Bilateral	Pelvis	Torso	Upper extremities - Bilateral	Head
Femoral head exc.	Pubic symphysis exc.	Sternum (mid at 6th rib height) exc.	Acromion exc.	CoG exc.
Patella exc.	Bilateral iliac crest exc.	C1-C7; T1-12; L1-L5 vertebra exc.	Olecranon exc.	Most Superior Point exc.
Distal tibia exc.	Bilateral ASIS exc.	Torso x, y, z angle	Distal radius exc.	Nasion exc.
Calcaneus exc.	Sacrum (Superior, Anterior & Posterior) exc.	Sternum velocity	Thumb distal phalanx exc.	Inion exc.
First distal phalanx exc.	Pelvic x, y, z angle	Upper Neck load	Distal humerus load	Bilateral Porion exc.
Distal femur load	Bilateral pubic rami load	Lower Neck load	Proximal humerus load	Bilateral Orbitale exc.
Proximal tibia load	Bilateral SI joint load	T12, L1-L5 Vertebra load	Distal forearm load	Head x, y, z angle
Distal tibia load	Bilateral ASIS load			CoG velocity

response induced by the altered posture. Signals with perfect correlation were assigned a perfect score (1), while signals with lower correlation were assigned values close to 0. The shape and amplitude of the responses were both weighted with 0.5. Signals with magnitude below the thresholds in Table 2, for both the nominal and the altered posture, were excluded from the analysis to focus the analysis on the more considerable effects. The thresholds were selected based on engineering judgement to avoid performing cross-correlation analysis between signals with poor signal-to-noise ratio.

Every group of compared OSPs included OSPs in which the posture of only one body region was varied. For every group of compared OSPs, the group's nominal OSP was used as the reference. For example, to quantify the influence of changing the lower extremity posture, the cross-correlation was performed for all OSPs that included variations of the lower extremity postures (#1 – #7, Appendix D Table D.1) against the nominal posture (#8, Appendix D Table D.1).

The next step was to use Root Mean Square (RMS) addition (Hovenga et al., 2005) to combine the cross-correlation value of all responses belonging to a body region into a single value representing the cross-correlation of an OSP's body region's response, Eqn (1). The combined cross-correlation of every OSP, belonging to an OSP-group was combined, Eqn (2), to calculate the influence of changing the posture of a body region to the response of a body region. Each body region was then weighted equally to calculate the effect of the OSP-group postures on the whole-body response, Eqn (3).

In order to interpret the variations highlighted by the cross-correlation analysis (low cross-correlation values), the corresponding signals were manually analyzed to understand the mechanism behind the altered responses.

Table 2
Amplitude threshold for including cross-correlation results in analysis.

Angle	Velocity	Displacement	Moment	Force
2° deg	1 m/s	50 mm	10 Nm	0.5 kN

$$CombCORA_{BODY-REGION-RESP,\ OSP} = 1 - \sqrt{\frac{\sum_{RESP=1}^{n} \left(1 - CORA_{RESP,OSP}\right)^2}{\mathrm{n}}} \quad (1)$$

$$CombCORA_{BODY-REGION-RESP,OSP-GROUP} = 1 - \sqrt{\frac{\sum_{OSP=1}^{k} \left(1 - CombCORA_{BODY-REGION-RESP,\ OSP}\right)^2}{k}} \quad (2)$$

$$WholeBody_{OSP-GROUP} = \frac{\sum_{BR=1}^{m} \left(CombCORA_{BODY-REGION-RESP,OSP-GROUP}\right)}{m} \quad (3)$$

Where,

$CORA_{RESP,OSP}$ is the CORA score of the response *RESP* for the *OSP*
n is the number of responses belonging to a body region
k is the number of OSPs belonging to an OSP group
m is the number of body regions

3. Results

The kinematics and kinetics cross-correlation between altered postures and nominal posture responses have been summarized in one color-coded (red for low-correlation scores and green for high correlation scores) table for each crash configuration: The Near-Side, Far-Side, and Frontal impact results can be seen in Tables 3–5, respectively. The results of Eqn (2) and (3) fill the cells of the tables with the cross-correlation of body region and whole-body responses, respectively. These tables highlight the body regions whose posture change had the largest influence on the response of a body region. The lower extremity posture had the largest overall influence in the lower extremities (with correlation score [0.35−0.47]), pelvis [0.61−0.7], and whole-body response [0.6−0.64], and had a large effect in the upper extremities [0.38−0.46]. The torso posture had the largest influence over the torso

Table 3
Near-Side Impact.

Response → / Posture ↓	Lower Extremities	Pelvis	Torso	Upper Extremities	Head	Whole-body
Lower Extremities	0.47	0.70	0.78	0.46	0.78	0.64
Torso Postures	0.85	0.84	0.62	0.53	0.46	0.66
Upper Extremities	0.86	0.90	0.85	0.45	0.88	0.79
Head postures	0.92	0.95	0.81	0.89	0.68	0.85

Table 4
Far-Side Impact.

Response → / Posture ↓	Lower Extremities	Pelvis	Torso	Upper Extremities	Head	Whole-body
Lower Extremities	0.42	0.66	0.77	0.46	0.84	0.63
Torso Postures	0.83	0.79	0.72	0.55	0.69	0.72
Upper Extremities	0.87	0.86	0.82	0.45	0.87	0.77
Head postures	0.93	0.94	0.87	0.82	0.77	0.87

Table 5
Frontal Impact.

Response → / Posture ↓	Lower Extremities	Pelvis	Torso	Upper Extremities	Head	Whole-body
Lower Extremities	0.35	0.61	0.78	0.38	0.90	0.60
Torso Postures	0.76	0.79	0.70	0.52	0.68	0.69
Upper Extremities	0.77	0.90	0.90	0.47	0.91	0.79
Head postures	0.90	0.93	0.88	0.84	0.79	0.87

0.30 0.40 0.50 0.60 0.70 0.80 0.90 1.00
Affected Response — Identical Response

and head responses for all tested impacts with correlation scores between [0.62–0.72], and [0.46–0.69], respectively. The upper extremity posture was mainly affecting the upper extremity responses, with correlation scores between [0.45–0.47], and [0.77–0.91], for the upper extremities and all other body regions, respectively. For the Far-Side impact, the upper extremities also influenced the torso response (with correlation score 0.82). The influence of the head's posture was limited to the head kinematics [0.68–0.79] and torso [0.81–0.88]. The torso

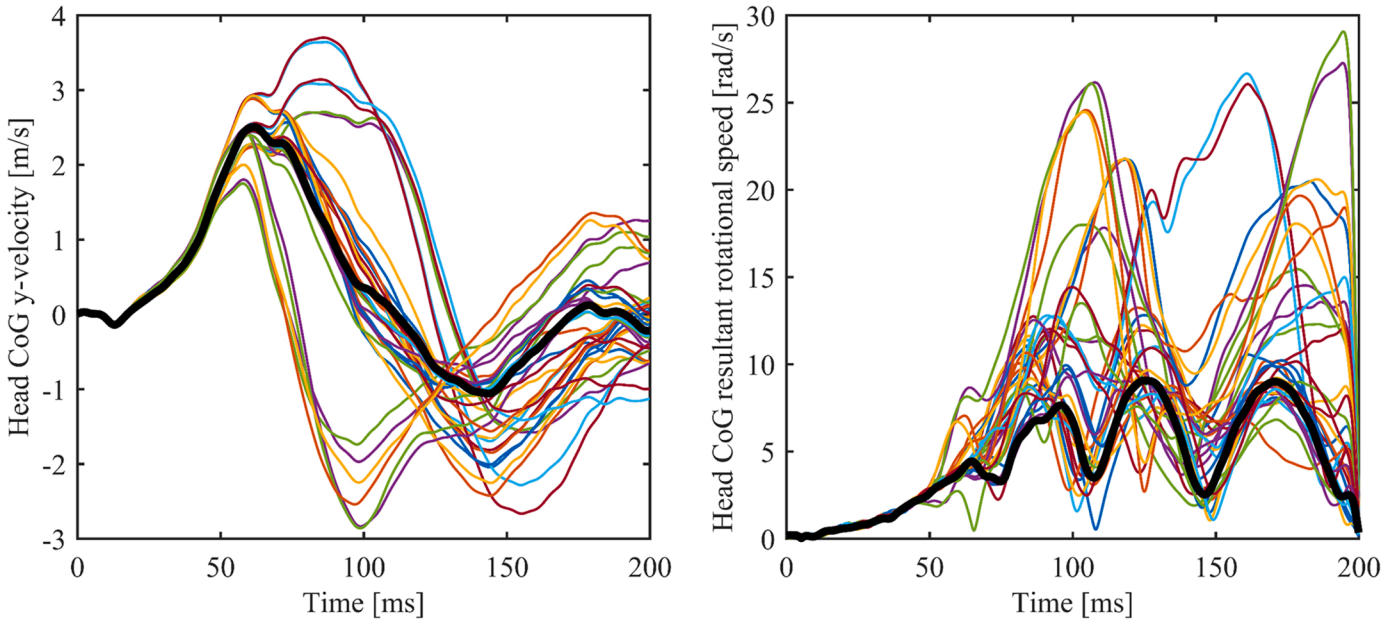

Fig. 4. Head relative lateral (left) and resultant rotational velocity (right) in the Near-Side impact, considering posture variation. The response of the nominal posture is highlighted with a thick black line.

responses, affected by the head posture, were mainly cervical spinal loads, such as the upper neck moment.

Also noteworthy was that the upper extremity responses seemed to be sensitive to most posture variations, with correlation scores between 0.38 and 0.89. Even variations in the head orientation influenced the upper extremity responses, with correlation scores between [0.82–0.89]. Excluding the head posture variations, would reduce the correlation of the upper extremity responses in the [0.38–0.55] range. Therefore, when evaluating the upper extremity kinematics and kinetics, the lower extremity and torso posture could play a comparably important role as the upper extremity postures.The head kinematics during the Near-Side impact are used to exemplify the large spread of occupant responses induced by posture variability. The maximum relative head lateral velocity and resultant rotational velocity (Fig. 4) range from 1.7 m/s to 3.7 m/s and from 8.7 rad/s to 19 rad/s, respectively, depending on the occupant posture, while assessing only the nominal posture would have predicted 2.5 m/s and 9.6 rad/s.

3.1. Lower extremities

The lower extremity postures had the overall largest influence in the whole-body response for all tested crash configurations. More specifically, besides the lower extremity responses, the pelvis kinematics were also altered, affecting the rest of the occupant's responses.

3.1.1. Near-side impact

The lower extremity postures lead to altered interaction with the vehicle's door panel, which affected the lower extremities loads. Locking the ankles with the right leg over the left ankle increased the right proximal tibia resultant force from 1.15 kN to 3.1 kN, the distal tibia resultant force from 0.9 kN to 2.5 kN, and the distal tibia resultant moment from 37 Nm to 68 Nm. Flexing the right knee also resulted in increased distal tibia moment (65 Nm). No major variations in the pelvis response were observed in the Near-Side impact. Finally, the interaction of the upper extremities with the interior was also affected. Crossing the legs over the left, changed the initial posture of the upper extremities, and increased the left and right proximal humerus moment from 16 Nm to 35 Nm and from 11 Nm to 30 Nm, respectively.

3.1.2. Far-side impact

The crossed legs posture affected the interaction with the vehicle's center console and door panel. Positioning the left leg over the right knee increased the torso rotation around the z-axis from 5° in the nominal posture to 15°.

Differences were observed between the crossed leg over-the-left and over-the-right knee, which may be connected to the interaction with the center console. When the left leg was over the right knee, the left arm was not supported by the center console during the crash phase, and as a result, larger excursions of the torso, head, and pelvis were observed.

Similarly, flexing one or both knees affected the lower extremities' interaction with each other and with the center console and showed altered kinematics for the lower extremities. When the right knee was flexed, the right leg impacted the left leg and pushed it toward the center console. When the left knee was flexed, the leg-leg interaction point changed, and load was transferred from the right knee to the left tibia, increasing the lower tibia resultant moment from 55 Nm to 80 Nm.

3.1.3. Frontal impact

Crossing the legs was the lower extremity posture that had the largest influence on the occupant response in the Frontal impact. It resulted in reduced pelvis restraint and increased lower extremity and torso excursions. Additionally, the peak tibia and femur moments were increased. The leg which was crossed under was generally subjected to higher loads. The left femur resultant moment was increased from 16 Nm in the nominal posture to 88 Nm when the right knee was crossed over the left. The crossed leg postures resulted in increased torso excursion (63 mm higher sternum x-excursion when crossing the legs over-the-left). It was also observed that when the upper extremities were placed over the crossed legs, the nominal upper extremity posture was altered, and they interacted with the frontal airbag and the occupant's chest.

Locking the ankles increased the lower tibia moment for the leg that was crossed over. The left tibia resultant moment was increased from 19 Nm in the nominal posture to 39 Nm when the left leg was crossed over the right ankle, and the right tibia resultant moment was increased from 20 Nm to 50 Nm when the right leg was crossed over the left ankle.

Flexing one or both knee(s) resulted in higher excursions for the lower extremities, mainly due to the increased distance from the glove compartment. The load transferred through the femur was also increased. The magnitude of the right femur force was increased from 0.7 kN in the nominal posture to 1.3 kN when the right knee was flexed.

The pelvis response was not considerably affected by flexing one knee or locking the ankles. However, flexing both knees or crossing the legs resulted in a less restrained pelvis that was able to move (Fig. 5) and rotate (Fig. 6) more. Crossing the legs (left or right) and flexing both knees resulted in increased pubic symphysis excursions (Fig. 5) and crossing the left leg over the right knee resulted in a maximum pelvic angle of 72° (Fig. 6). The resultant force through the L5 vertebra was reduced by 45 % and 64 % compared to the nominal posture (1.1 kN) when the legs were crossed over the left and right, respectively. No submarining was observed, however the pelvic angle and pubic symphysis movement indicate that crossing the legs can result in conditions that are closer to the submarining threshold, by rotating the pelvis backward.

3.2. Torso

The torso posture had the largest influence on the torso and head responses for all tested crash pulses.

3.2.1. Near-side impact

In the Near-Side impact, the torso posture had the largest influence on the head kinematics. Changing posture in the coronal plane influenced the contact time of the head with the inflatable curtain. When the occupant was leaning inboard, the head built up more relative speed

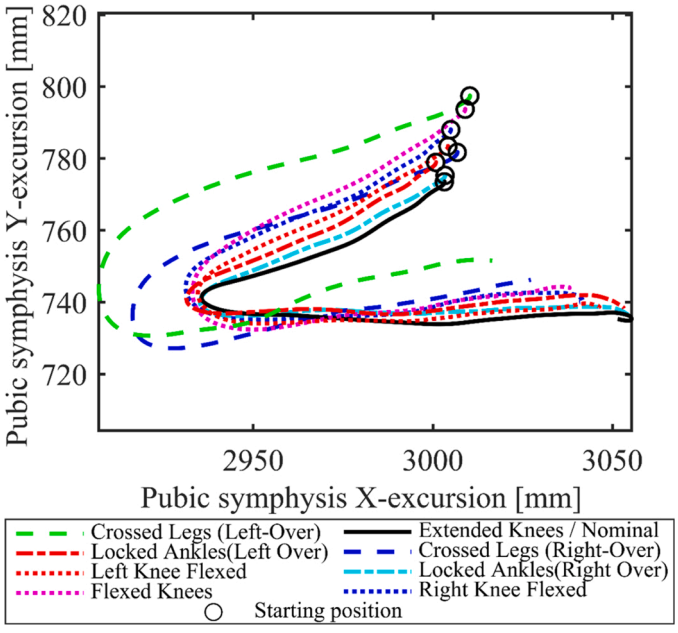

Fig. 5. Pelvis trajectory during the Frontal impact for all OSPs with varied lower extremity posture.

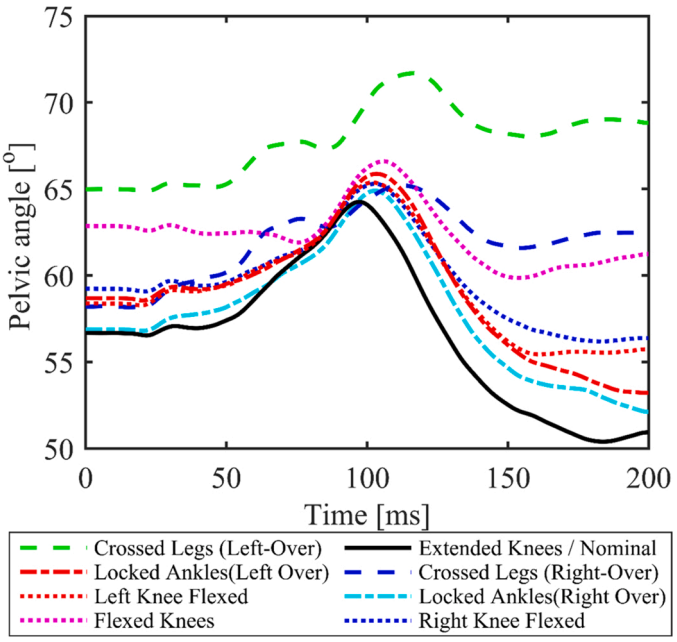

Fig. 6. Pelvic angle during the Frontal impact. Changing the lower extremity posture affected both the initial pelvic angle and the pelvic angle response.

(3.1 m/s compared to 2.5 m/s in the nominal posture), because of the increased distance to the inflatable curtain. Additionally, the head rotation was sensitive to the occupant's torso posture. The head rotational velocity around the z-axis ranged from 11.8 rad/s in the nominal posture up to 28.4 rad/s while leaning inboard. The peak head yaw-angle was increased from -8° in the nominal posture to -31° when leaning inboard and to 30° when leaning outboard. Moreover, the lower neck resultant moment was increased when the occupant was leaning forward or outboard. When leaning forward and outboard, the moment was 82 Nm compared to 14 Nm in the baseline. When the occupant was semi-reclined, the head and torso response were less sensitive to the coronal torso posture due to the added support from the seat side-bolsters.

3.2.2. *Far-side impact*

The torso posture had a large influence on the head kinematics during the Far-Side impact. In this situation when the occupant was leaning outboard, the distance to the center console was increased, and higher relative speed was built up before the occupant was restrained. The peak relative y-velocity was 3.8 m/s when in the nominal posture, increased to 4.6 m/s when leaning outboard, and reduced to 3.2 m/s when leaning inboard. The occupant's increased kinetic energy resulted in larger excursions for the torso, pelvis, head, and upper extremities. The head rotational velocity was increased when leaning forward or outboard (Fig. 7). This was more pronounced with the occupant leaning outboard and forward, in which case, the head peak-to-peak z-rotational velocity increased from 19 rad/s to 36.5 rad/s. Simulations with semi-reclined occupant showed lower head rotational velocities and were less sensitive to variations due to the torso leaning in the coronal plane (Fig. 7).

3.2.3. *Frontal impact*

When the occupant was semi-reclined, the sternum excursion was increased by up to 17 mm, but the peak longitudinal position did not exceed the sternum position of the nominal posture. However, forward-leaning as well as outboard-leaning occupants exhibited a peak longitudinal position that was increased by up to 25 mm compared to the nominal (Fig. 8). Additionally, positioning the occupant in the forward-leaning posture produced larger torso rotations around the z-axis (from

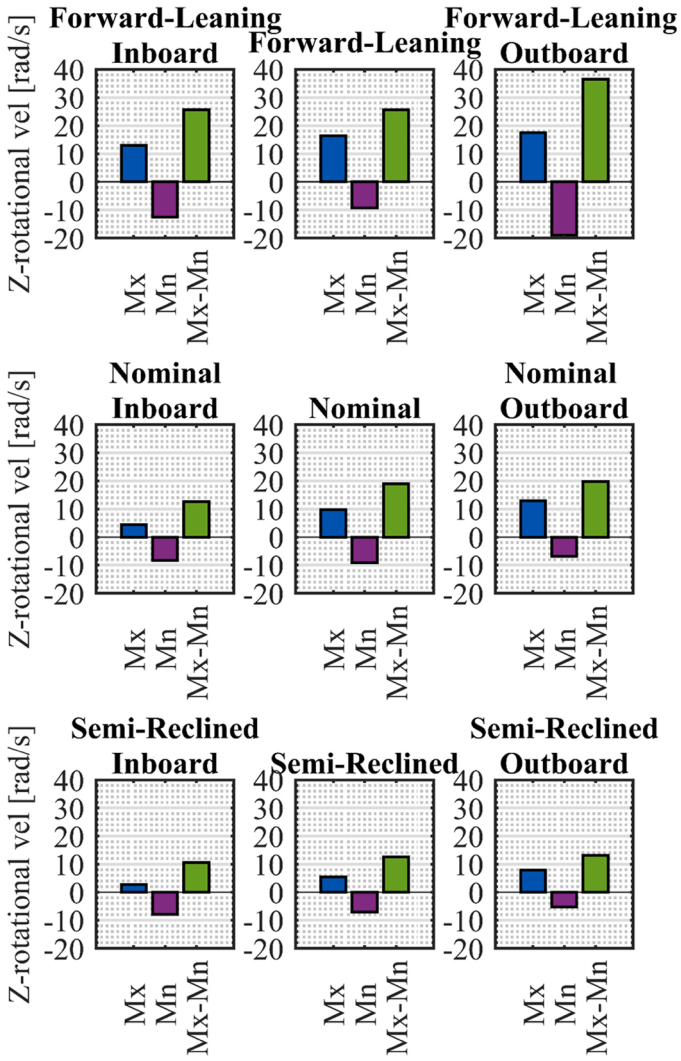

Fig. 7. Maximum (Mx), minimum (Mn), and maximum-minimum (Mx-Mn) head rotational velocity in the Far-Side impact for OSPs with varied torso posture.

7° to 30° when leaning forward and inboard simultaneously). The head also rotated further, earlier in the crash phase, and the lower neck resultant moment was reduced from 75 Nm to 45 Nm. Altered interaction between the upper extremities and the door panel were also observed while the occupant was leaning forward as well as backward. Leaning backward reduced the right distal forearm resultant force from 0.7 kN to 0.5 kN and increased the left distal forearm resultant force from 0.73 kN to 0.85 kN.

The lumbar responses were altered depending on the torso posture. Leaning backward increased the L5 resultant force from 1.1 kN to 1.3 kN, and leaning forward, reduced the force to 0.9 kN. Leaning outboard had a similar effect with increased lumbar loads (1.25 kN).

3.3. *Upper extremities*

The upper extremity posture predominantly influenced the upper extremity responses and, in the Far-Side impact, also affected the torso kinematics.

3.3.1. *Near-side impact*

Using the armrest in the door as support while leaning outboard or being in the nominal posture in the coronal plane, resulted in a more gradual coupling with the door panel and decreased the z-rotation of the

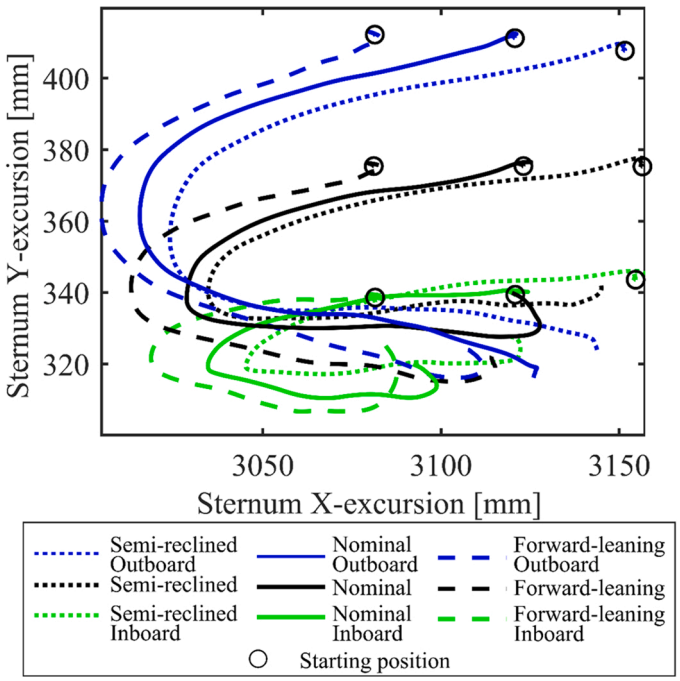

Fig. 8. Sternum (at the height of the 6th rib) excursions during the Frontal impact for OSP with different torso posture.

torso by 4° and the head by 6°. On the contrary, crossing the arms over the chest increased the distance to the door panel and the sternum z-rotation by 4°. Finally, the torso y-excursion was increased by 20 mm when holding the phone, and the right distal forearm resultant moment was increased from 18 Nm to 32 Nm.

3.3.2. Far-side impact

The interaction of the upper extremities with the center console was affected when the occupant was using the center console as a support or crossing the arms over the chest. The reduced coupling with the center console allowed for larger excursions of the torso, pelvis, and head. The torso rotated 7° more around the x-axis, and the head moved 40 mm further inboard. Crossing the arms over the chest had a similar effect (35 mm higher lateral head excursion). In the scenario where the occupant was leaning inboard, it was observed that the torso movement was affected by using the center console armrest. Therefore, the interaction with the center console could be important to prevent belt slip-out. More specifically, the torso rotated up to 9° more around the x-axis (Fig. 9) when supporting the left upper extremity on the center console or crossing the arms, and the longitudinal excursion of the torso was increased by 9 mm, especially while leaning inboards. The torso forward excursion was also increased by using the center console for all torso postures (Fig. 9). Finally, holding the phone had minor effects on the occupant's kinematics but increased the right distal forearm resultant moment from 23 Nm to 40 Nm.

3.3.3. Frontal impact

During the Frontal impact, the interaction with the center console was the main aspect that affected the occupant's response. Supporting the left elbow on the center console increased the left humerus proximal resultant moment from 13 to 22 Nm and increased the sternum y-excursion by 10 mm. When the occupant was supporting the right elbow on the door armrest, the torso rotated 8° more around the z-axis. The torso rotation also affected the head rotation, which rotated 7° in the opposite direction. The posture of holding a phone (in the right hand) increased the right humerus resultant moments from 12 Nm to 32 Nm and forearm resultant moment from 24 Nm to 36 Nm.

3.4. Head

The head orientation affected mainly the head kinematics and the upper neck loads. In the Frontal impacts, rotating the head affected the upper neck loads. Rotating the head to the right (80°) increased the upper neck resultant moment from 14 Nm to 27 Nm. In the Far-Side impact, the upper neck moment was also affected. Rotating the head to the right (55°) increased the upper neck resultant moment from 34 Nm to 41 Nm, and rotating to the left reduced the moment to 30 Nm. Lastly, in the Near-Side impact, rotating the head to the left or right reduced the upper neck resultant moment from 17 Nm to 7 Nm and 11 Nm, respectively.

4. Discussion

Real-world crashes can occur in a multitude of crash configurations, involving occupants seated in different postures. On the contrary, standardized crashworthiness assessment is performed with standardized crash configurations and sitting postures. For this study, a systematic investigation into the effects of the different occupant postures was performed, contributing to the identification of postures that could potentially pose safety challenges. An extensive set of occupant postures beyond standardized crashworthiness assessment have been evaluated. Three crash configurations, covering diverse car-car crashes that could occur at intersections, have been simulated.

The postures used in this study aimed at covering a wide range of occupant sitting postures that could be expected in real-world situations, including different postures of multiple body regions. Due to the computational time required, a full factorial design where postures of all body regions would have been combined, was not considered possible. A manual selection of the occupant sitting postures was performed, covering a wide range of postures reported in the literature.

The cross-correlation analysis indicates that the postures of the lower extremities had the largest influence on the whole-body response for all evaluated crash pulses. The conclusion that the lower extremity postures have the largest influence in the whole-body responses could be affected by the equal weighing of the body region responses (Eqn (3)) as well as by the responses selected and the thresholds (Table 2) used in the analysis. Bose et al. (2010) investigated the effects of lower extremity postures by flexing and extending the knees and concluded that they had a minor influence, mainly on the response of the lower extremities. In the present study, the inclusion of the crossed leg postures, the most influential lower extremity posture, could explain the discrepancy in the conclusions. Additionally, using a FE HBM compared to a multibody model, may have produced visible secondary effects of the OSPs, such as altered pelvic angles for different postures, and may also have improved the prediction of the interaction with the restraint system. Even though the HBM used in this study has been validated for multiple impact conditions, it should be noted that limited data exist to evaluate the biofidelity of non-nominal postures as of today.

In this study, dependence was observed between the posture definitions of different body regions. When, for example, the upper extremity posture is defined relative to the lower extremity posture, it is difficult to isolate the source of the variation since multiple parameters are affected simultaneously. This was seen in the Frontal impact simulations, in which crossing the legs resulted in a different initial posture of the upper extremities and introduced interaction between the frontal airbag, arms, and the chest. Furthermore, changing the lower extremity posture affected the initial pelvic angle (Fig. 6). Therefore, the altered kinematics induced by the crossed leg postures are difficult to interpret, as they could be (partially) attributed to the changed initial pelvic angle. Izumiyama et al. (2018) identified the pelvic angle as an important factor for predicting the pelvis kinematics and even observed deviation in the head and neck injury measures as it was changed. Even though no submarining was observed in any of the simulations, the increased initial pelvic angle observed, when the occupant was sitting with crossed

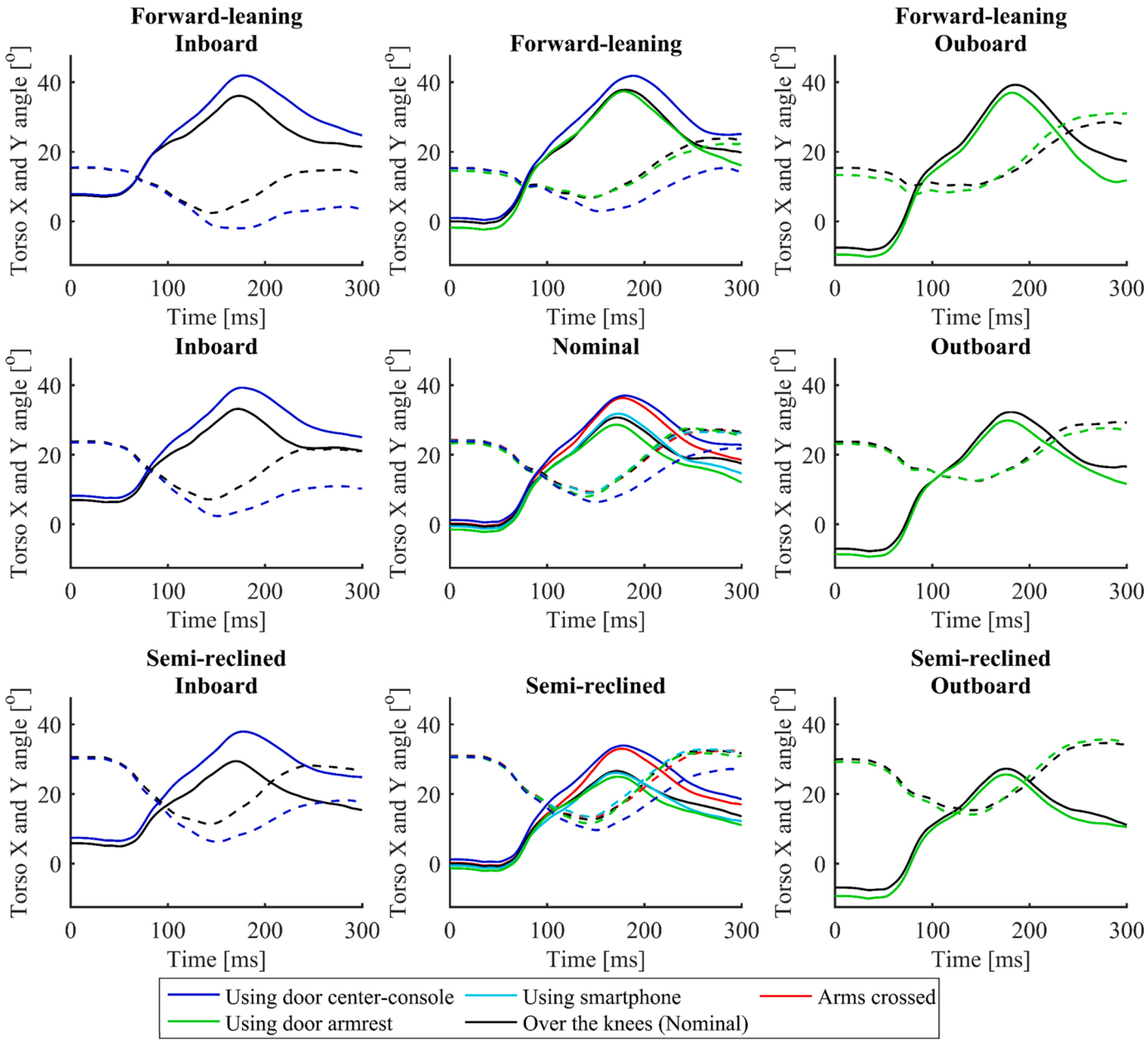

Fig. 9. Torso X-angle (lateral direction, solid line) and Y-angle (longitudinal direction, dashed line) during the Far-Side impact are visualized for all torso and upper extremity postures.

legs (Fig. 6), could be linked to an increased submarining risk as larger pelvis angle is associated with larger risk of submarining (Uriot et al., 2015).

This study benefits from the occupant positioning through pre-simulation since the occupant's biomechanical properties, such as joint stiffness, are respected during positioning, compared to some morphing techniques, which would ignore such properties. The HBM, used in the present study, has been evaluated in a wide range of in-crash and pre-crash events. However, due to lack of data, the biofidelity of the model's biomechanical properties has not been assessed in conditions such as low-force joint manipulation to alter the posture. Evaluating the biofidelity of the dependence between body regions, such as establishing pelvic orientation data and spinal alignment for different sitting postures of individuals, would be beneficial for assessing the success of the positioning method. At the same time, assuming that the posture of a body region not being dependent on other body region postures, and over specifying the orientation and position of anatomical landmarks, might not be the best representation of the occupant postures seen in the real world.

The torso and the head responses were considerably affected by the torso posture for all crash pulses tested. The observed head kinematics, when the occupant was leaning inboard during the Frontal impact, are comparable to the observations of Donlon et al. (2020) for frontal impacts. In this study, the maximum longitudinal head excursion was increased by 35 mm compared to the reported 45–70 mm (Donlon et al., 2020), and the maximum resultant velocity of the head was increased in both studies. Differences were observed in the lateral kinematics. In the present study, the occupant was pushed inboard instead of outboard, most likely because of the different crash pulses used (frontal-oblique vs. pure-frontal). The test environment used, as well as the occupant leaning angle (-7° vs.−21°), may also have an influence, explaining some of the observed divergences.

The torso postures had a considerable effect on the occupant movement during side impacts. Leaning inboard during the Near-Side impact or outboard during Far-Side impact increased the distance with the vehicle interior (door panel and center console) and allowed for higher relative head velocities. Additionally, for the Far-Side impact, the upper extremities affected the interaction with the center console and, consequently, the torso and head lateral displacement. In contrast, the newly introduced assessment protocol for far-side impacts (European New Car Assessment Programme (Euro NCAP, 2020b) is utilizing the WorldSID 50th Male ATD, which does not include the forearm region.

For semi-reclined occupants, an increase in the lumbar force was observed during the Frontal impact. During side-impacts, the occupant response was less sensitive to the torso posture in the coronal plane when semi-reclined. In contrast, leaning forward was shown to affect the occupant's movement and response considerably, as also found by Hwang et al. (2016). During side and frontal impacts, increased head rotations and cervical spinal loads were observed for the forward-leaning posture. Those findings draw attention to the occupant's movement during pre-crash maneuvers, which could alter the occupant's pre-impact posture. Some of the postures used in the present study, such as the (forward/inboard/outboard) leaning torso postures, could be considered as the result of a pre-crash maneuver. The selected initial leaning inboard torso postures were comparable with the findings of Reed et al. (2021) for maximum head excursion during braking and left/right lane change maneuvers. However, it should be noted that pre-crash occupant kinematics could influence additional parameters of the occupant's state (muscle bracing level, velocity relative to the vehicle, and others) and consequently affect the occupant's injury risk.

The simulations in this study were performed with a HBM of average male adult shape and size, due to fact that this model has been evaluated in a wide array of pre-crash and in-crash conditions. The seat was always adjusted in the mid-fore/aft position to limit the varied parameters, using a seat configuration compatible with standardized testing, and the belt was routed to the shortest path. Contrary to this, Reed et al. (2020a) reported that the seat was frequently adjusted behind the mid-for/aft position and non-ideal belt fit was observed more than 35 % of the time. As an example, observed from the present study, the shoulder belt was placed distal on the clavicle for the inboard leaning occupant even when the belt was routed to the shortest path. Additional aspects such as individual anatomical variations, variations across the sexes, and various anthropometries, that could affect both the occupant posture, seat position selection, belt fit, and their influence on occupant responses, were outside the scope of this study.

The findings of this study, such as the influence of the crossed legs posture to the pelvis response and the sensitivity of the head kinematics due to altered torso posture, could be affected by occupants of different shape and size. The knee-to-dashboard contact could be affected by either occupants of different size or by changing the seat fore/aft position. Adjusting the seat behind the mid-for/aft position or replacing the passenger with an occupant of shorter stature, could reduce or delay the knee-to-dashboard contact, and further change the interaction with the lap belt. Additionally, the lap belt interaction could be affected due to several parameters, such as the amount of fat and its distribution in the abdominal area or even by slack in the belt introduced by choice of clothes. The changed interaction with the vehicle interior could exaggerate the results found for different population groups, such as shorter occupants or occupants of higher BMI. Investigating the generality of the results of the current study, while considering the aforementioned aspects, would be of value to ensure that the development efforts target the protection of occupants in real-world conditions and could facilitate enhanced occupant protection.

Employing numerical simulations with HBMs enables the possibility of investigating occupants' postures compared to other tools traditionally used in vehicle crashworthiness assessment, such as ATDs, which cannot be positioned in the postures investigated in this study. Gierczycka et al. (2015) published a comparative study about the sensitivity of HBMs and ATDs in arm positions during side impact, in which the HBM, in contrast to the ATD, demonstrated significant sensitivity to different arm positions. In another study (Forman et al., 2019), a preliminary assessment of ATDs and HBMs as tools for examining restraint interaction, occupant kinematics, and occupant protection in reclined seats was performed, and the HBM was found to be suitable for being positioned in reclined postures that the ATD could not achieve. Further studies are needed to evaluate the biofidelity of HBMs in reclined and non-nominal postures. The kinematic and kinetic results presented in the current study may be considered as indicators of increased injury risk. To be able to utilize HBMs at their full potential, tissue-level injury criteria for more body regions (such as the upper and lower extremities) would be beneficial.

The presented study contributes by quantifying the effects of occupants' posture variations on kinematic and kinetic responses during predicted intersection crashes. The influence of the lower extremities and torso postures highlights that evaluating occupant safety and developing protection systems while considering postures beyond the nominal has the potential to enhance real-world occupant safety. Considering several postures highlighted in this study as potentially challenging for developing protection systems, could support the development of more robust restraint systems and consequently enhance the real-world occupant protection capabilities.

5. Conclusions

With the purpose of investigating the influence of a wide range of occupant postures under diverse impact conditions, a cross-correlation method was applied on simulation results which was effective for systematically quantifying the effect of altered postures.

The lower extremities were identified as the body region, which could considerably affect the whole-body response for all the evaluated crash configurations. In frontal impacts, crossing the legs can affect the lower extremities to vehicle interior and the lap-belt to pelvis interaction resulting in altered pelvis kinematics, and consequently, whole-body kinematics.

Additionally, the torso posture influenced the response of the torso and head, particularly in side impacts. Changing the torso posture in the coronal plane was the most influential parameter for the torso and head responses during side impacts. Leaning away from the struck side of the vehicle increased the head to vehicle relative velocity.

This study suggests that leaning forward can pose more safety challenges for occupant protection than moderately leaning backward. The forward-leaning occupant posture was more sensitive to variations of the torso coronal posture compared to the semi-reclined occupant posture which was supported more by the seat side bolsters.

In far-side impacts, the interaction between the occupant's left upper extremity and the vehicle's center console affected the torso kinematics. Supporting the left arm on the center console was found to increase the longitudinal and lateral torso excursions.

Declaration of competing interest

Leledakis, Östh, and Jakobsson are employees of Volvo Car Corporation.

CRediT authorship contribution statement

Alexandros Leledakis: Conceptualization, Methodology, Software, Formal analysis, Investigation, Data curation, Writing - original draft, Visualization. **Jonas Östh:** Conceptualization, Methodology, Supervision, Writing - review & editing. **Johan Davidsson:** Supervision, Writing - review & editing. **Lotta Jakobsson:** Conceptualization, Methodology, Supervision, Writing - review & editing.

Acknowledgments

The work was carried out at SAFER Vehicle and Traffic Safety Centre at Chalmers University of Technology, Gothenburg, as part of The European Union Horizon 2020 Research and Innovation Programme Project, OSCCAR. OSCCAR has received funding from the European Union Horizon 2020 Research and Innovation Programme under Grant Agreement No 768947.

The authors would like to thank the participants of OSCCAR WG3, especially Martin Östling at Autoliv Research, for the fruitful discussions during the project meetings. The content of this publication does not reflect the official opinion of the European Union. Responsibility for the information and views expressed therein lies entirely with the authors.

Appendix A–F Supplementary data

Supplementary data associated with this article can be found, in the online version, at doi:https://doi.org/10.1016/j.aap.2021.106170.

References

Bingley, L., Richard, M., Gabrielle, C., 2005. Determination of real world occupant postures by photo studies to aid smart restraint development. Proceedings of the 19th International Technical Conference on the Enhanced Safety of Vehicles (ESV), Paper No 05-0319.

Bohman, K., Jakobsson, L., Nurbo, P., Olander, A., Andersson, A., 2020a. Lateral movement of front seat passengers in everyday traffic. Proceedings of the International Research Council on the Biomechanics of Injury (IRCOBI) 2020. Paper No IRC-20-53.

Bohman, K., Örtlund, R., Kumlin Groth, G., Nurbo, P., Jakobsson, L., 2020b. Evaluation of users' experience and posture in a rotated swivel seating configuration. Traffic Inj. Prev. https://doi.org/10.1080/15389588.2020.1795149.

Bose, D., Crandall, J.R., Untaroiu, C.D., Maslen, E.H., 2010. Influence of pre-collision occupant parameters on injury outcome in a frontal collision. Accid. Anal. Prev. 42 (4), 1398–1407. https://doi.org/10.1016/j.aap.2010.03.004.

Donlon, J.-P., Richardson, R., Jayathirtha, M., Forman, J., Kerrigan, J., Kent, R., Arbogast, K.B., Maripudi, V., Scavnicky, M., 2020. Kinematics of inboard-leaning occupants in frontal impacts. Traffic Inj. Prev. 21 (4), 272–277. https://doi.org/10.1080/15389588.2020.1745787.

European New Car Assessment Programme (Euro NCAP), 2020a. MPDB Frontal Impact Testing Protocol Version 1.1.1. Available at: https://cdn.euroncap.com/media/55858/euro-ncap-mpdb-testing-protocol-v111.pdf. Accessed 15 January 2021.

European New Car Assessment Programme (Euro NCAP), 2020b. Far Side Occupant Test & Assessment Procedure Version 2.0.1. Available at: https://cdn.euroncap.com/media/58231/euro-ncap-far-side-test-and-assessment-protocol-v201.pdf. Accessed 15 January 2021.

Fice, J.B., Blouin, J.-S., Siegmund, G.P., 2018. Head postures during naturalistic driving. Traffic Inj. Prev. 19 (6), 637–643. https://doi.org/10.1080/15389588.2018.1493582.

Forman, J., Lin, H., Gepner, B., Wu, T., Panzer, M., 2019. Occupant safety in automated vehicles. Int. J. Automot. Eng. 10 (2), 139–143. https://doi.org/10.20485/jsaeijae.10.2_139.

Gabler, L.F., Crandall, J.R., Panzer, M.B., 2016. Assessment of kinematic brain injury metrics for predicting strain responses in diverse automotive impact conditions. Ann. Biomed. Eng. https://doi.org/10.1007/s10439-016-1697-0.

Gehre, C., Stahlschmidt, S., 2011. Assessment of dummy models by using objective rating methods. Proceedings of the 22nd International Technical Conference on the Enhanced Safety of Vehicles (ESV) 11–0216.

Ghaffari, G., Brolin, K., Bråse, D., Pipkorn, B., Svanberg, B., Jakobsson, L., Davidsson, J., 2018. Passenger kinematics in lane change and lane change with braking manoeuvres using two belt configurations: standard and reversible pre-pretensioner. Proceedings of the International Research Council on the Biomechanics of Injury (IRCOBI) 2018. Paper No IRC-18-80.

Gierczycka, D., Cronin, D.S., 2017. Occupant thorax response variations due to arm position and restraint systems in side impact crash scenarios. Accid. Anal. Prev. 106, 173–180. https://doi.org/10.1016/j.aap.2017.05.017.

Gierczycka, D., Watson, B., Cronin, D., 2015. Investigation of occupant arm position and door properties on thorax kinematics in side impact crash scenarios-comparison of ATD and human models. Int. J. Crashworthiness 20 (3), 242–269. https://doi.org/10.1080/13588265.2014.998000.

Hovenga, P.E., Spit, H.H., Uijldert, M., Dalenoort, A.M., 2005. Improved Prediction of Hybrid-iii Injury Values Using Advanced Multibody Techniques and Objective Rating. SAE Technical Paper 2005-01-1307. https://doi.org/10.4271/2005-01-1307.

Hwang, E., Hu, J., Chen, C., Klein, K.F., Miller, C.S., Reed, M.P., Rupp, J.D., Hallman, J. J., 2016. Development, evaluation, and sensitivity analysis of parametric finite element whole-body human models in side impacts. Stapp Car Crash J. 2016 (60), 473–508. PMID: 27871104.

Iraeus, J., Pipkorn, B., 2019. Development and validation of a generic finite element ribcage to be used for strain-based fracture prediction. Proceedings of the International Research Council on the Biomechanics of Injury (IRCOBI) 2019. Paper No IRC-19-35.

Izumiyama, T., Nishida, N., Iwanaga, H., Chen, X., Ohgi, J., Mori, K., Hayashi, T., Sakuramoto, I., Asahi, R., Sugimoto, S., Ueno, M., 2018. The analysis of an individual difference in human skeletal alignment in seated posture and occupant behavior using HBMs. Proceedings of the International Research Council on the Biomechanics of Injury (IRCOBI) 2018. Paper No IRC-18-84.

Koppel, S., Jiménez Octavio, J., Bohman, K., Logan, D., Raphael, W., Quintana Jimenez, L., Lopez-Valdes, F., 2019. Seating configuration and position preferences in fully automated vehicles. Traffic Inj. Prev. 20 (sup2), 103–109. https://doi.org/10.1080/15389588.2019.1625336.

Larsson, K.J., Pipkorn, B., Iraeus, J., Bolte, J.H., Agnew, A.M., Hu, J., Reed, M.P., Sunnevång, C., 2019. Evaluation of the benefits of parametric human body model morphing for prediction of injury to elderly occupants in side impact. Proceedings of the International Research Council on the Biomechanics of Injury (IRCOBI) 2019. Paper No IRC-19-33.

Leledakis, A., Lindman, M., Östh, J., Wågström, L., Davidsson, J., Jakobsson, L., 2021. A method for predicting crash configurations using counterfactual simulations and real-world data. Accid. Anal. Prev. 150, 105932 https://doi.org/10.1016/j.aap.2020.105932.

Mroz, K., Östling, M., Richardson, R., Kerrigan, J., Forman, J., Gepner, B., Lubbe, N., Pipkorn, B., 2020. Effect of seat and seat belt characteristics on the lumbar spine and pelvis loading of the SAFER human body model in reclined postures. Proceedings of the International Research Council on the Biomechanics of Injury (IRCOBI) 2020. Paper No IRC-20-58.

Nie, B., Crandall, J.R., Panzer, M.B., 2017. Computational investigation of the effects of knee airbag design on the interaction with occupant lower extremity in frontal and oblique impacts. Traffic Inj. Prev. 18 (2), 207–215. https://doi.org/10.1080/15389588.2016.1219728.

Nie, B., Gan, S., Chen, W., Zhou, Q., 2020. Seating preferences in highly automated vehicles and occupant safety awareness: a national survey of Chinese perceptions. Traffic Inj. Prev. 21 (4), 247–253. https://doi.org/10.1080/15389588.2020.1738013.

Ólafsdóttir, J.M., Östh, J.K.H., Davidsson, J., Brolin, K.B., 2013. Passenger kinematics and muscle responses in autonomous braking events with standard and reversible pre-tensioned restraints. Proceedings of the International Research Council on the Biomechanics of Injury (IRCOBI) 2013. Paper No IRC-13-70.

Östh, J., Olafsdóttir, J.M., Davidsson, J., Brolin, K., Östh, J., Ólafsdóttir, J.M., Davidsson, J., Brolin, K., 2013. Driver Kinematic and Muscle Responses in Braking Events With Standard and Reversible Pre-tensioned Restraints: Validation Data for Human Models. SAE Technical Paper 2013-22-0001. https://doi.org/10.4271/2013-22-0001.

Östh, J., Bohman, K., Jakobsson, L., 2020. Evaluation of kinematics and restraint interaction when repositioning a driver from a reclined to an upright position prior to frontal impact using active human body model simulations. Proceedings of the International Research Council on the Biomechanics of Injury (IRCOBI) 2020. Paper No IRC-20-50.

Park, G., Kim, T., Panzer, M.B., Crandall, J.R., 2016. Validation of shoulder response of human body finite-element model (GHBMC) under whole body lateral impact condition. Ann. Biomed. Eng. 44 (8), 2558–2576. https://doi.org/10.1007/s10439-015-1546-6.

Pipkorn, B., Larsson, K.J., Rapela, D.P., Markusic, C., Whitcomb, B., Ayyagari, M., Sunnevång, C., 2018. Occupant protection in far-side impacts. Proceedings of the International Research Council on the Biomechanics of Injury (IRCOBI) 2018. Paper No IRC-18-16.

Pipkorn, B., Iraeus, J., Björklund, M., Bunketorp, O., Jakobsson, L., 2019. Multi-scale validation of a rib fracture prediction method for human body models. Proceedings of the International Research Council on the Biomechanics of Injury (IRCOBI) 2019. Paper No IRC-19-34.

Poulard, D., Subit, D., Donlon, J.-P., Lessley, D.J., Kim, T., Park, G., Kent, R.W., 2014. The contribution of pre-impact spine posture on human body model response in whole-body side impact. Stapp Car Crash J. 58, 385–422. PMID: 26192961.

Poulard, D., Subit, D., Donlon, J.-P., Kent, R.W., 2015a. Development of a computational framework to adjust the pre-impact spine posture of a whole-body model based on cadaver tests data. J. Biomech. 48 (4), 636–643. https://doi.org/10.1016/j.jbiomech.2014.12.050.

Poulard, D., Subit, D., Nie, B., Donlon, J.-P., Kent, R.W., 2015b. The contribution of pre-impact posture on restrained occupant finite element model response in frontal impact. Traffic Inj. Prev. 16 (sup2), S87–S95. https://doi.org/10.1080/15389588.2015.1064529.

Reed, Matthew P., Ebert, S.M., Jones, M.L.H., Hallman, J.J., 2020a. Prevalence of non-nominal seat positions and postures among front-seat passengers. Traffic Inj. Prev. https://doi.org/10.1080/15389588.2020.1793971.

Reed, Matthew P., Ebert, S.M., Jones, M.L.H., 2020b. Naturalistic Passenger Behavior: Postures and Activities, Technical Report UMTRI-2020-2. University of Michigan Transportation Research Institute, Ann Arbor, MI.

Reed, M.P., Ebert, S.M., Jones, M.L.H., Park, B.-K., 2021. Occupant Dynamics During Crash Avoidance Maneuvers. (Report No. DOT HS 812 997). National Highway Traffic Safety Administration.

Schneider, L.W., Robbins, D.H., Pflueg, M.A., Snyder, R.G., 1983. Development of Anthropometrically Based Design Specifications for an Advanced Adult Anthropomorphic Dummy Family, Volume 1, Final Report UMTRI-83-53-1. University of Michigan Transportation Research Institute, Ann Arbor, MI.

Uriot, J., Potier, P., Baudrit, P., Trosseille, X., Richard, O., Douard, R., 2015. Comparison of HII, HIII and THOR dummy responses with respect to PMHS sled tests. Proceedings of the International Research Council on the Biomechanics of Injury (IRCOBI) 2015. Paper No IRC-15-55.

Wågström, L., Kling, A., Norin, H., Fagerlind, H., 2013. A methodology for improving structural robustness in frontal car-to-car crash scenarios. Int. J. Crashworthiness 18 (4), 385–396. https://doi.org/10.1080/13588265.2013.801292.

Yoganandan, N., Arun, M.W.J., Stemper, B.D., Pintar, F.A., Maiman, D.J., 2013. Biomechanics of human thoracolumbar spinal column trauma from vertical impact loading. Ann. Adv. Automot. Med. 2013 (57), 155–166. PMID: 24406955.

Zhang, L., Chen, L., Vertiz, A., Balci, R., 2004. Survey of Front Passenger Posture Usage in Passenger Vehicles. SAE Technical Paper 2004-01-0845. https://doi.org/10.4271/2004-01-0845.

Appendix A. Restraint system timing

The timing of the restraint systems that were used for the Near-Side, Far-Side, and Frontal crash simulations were based on engineering judgement and can be seen in Table A.1.

Table A.1 Timing of the restrain systems for every crash configuration.

	Near-Side	Far-Side	Frontal
Belt pretensioner	40ms	25ms	10ms
Passenger Frontal Airbag	40ms	25ms	15ms
Inflatable Curtain Airbag	40ms	-/-	-/-
Torso Side Airbag	40ms	-/-	-/-

Appendix B. Validation of the interior and restraint FE model

To validate the passenger compartment model, a simulation with the Hybrid-III ATD positioned in the front passenger seat was performed and compared with a full-scale crash test that was performed at Volvo Cars Safety Centre, Figure B1. The load case simulated and tested was an Offset Deformable Barrier (ODB) impact at 64 km/h, and the simulation data matched the test data well in phase and relatively well in magnitude, leading to the conclusion that the passenger compartment model is a good representation of a real vehicle environment.

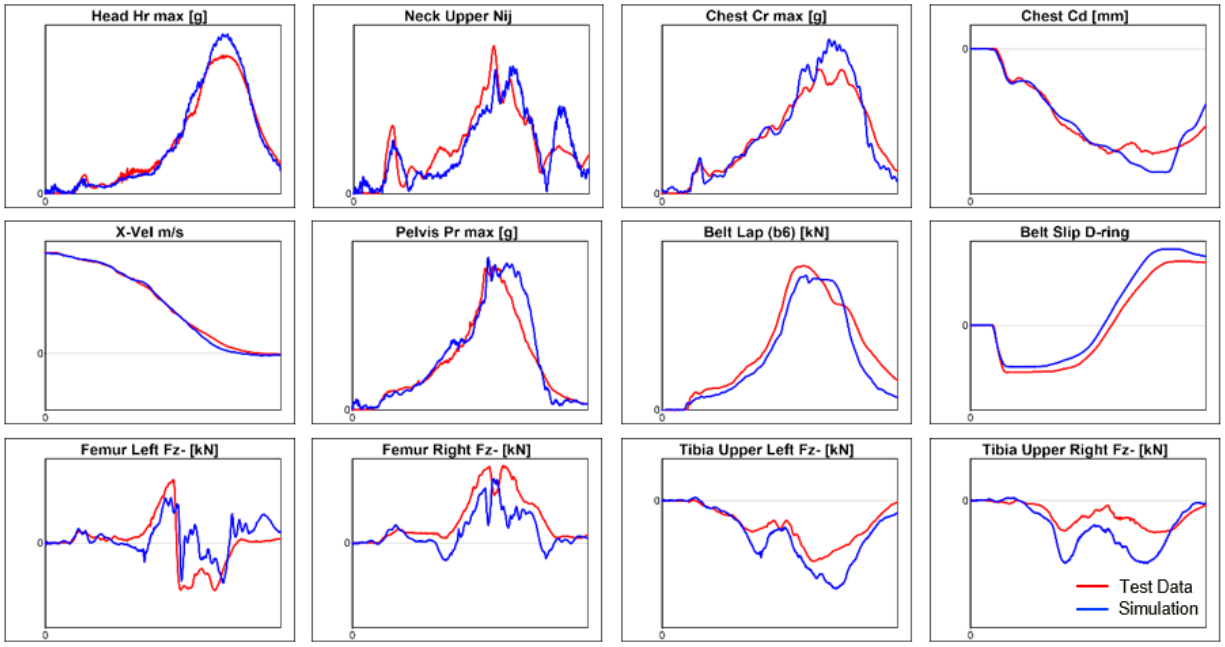

Figure B.1 A simulation with a Hybrid-III ATD positioned in the front passenger seat was compared with a full-scale crash test in an Offset Deformable Barrier impact at 64km/h.

Appendix C. Crash Configurations

The selected crash configurations (Fig C.1) are representative of predicted crashes in urban intersections (Leledakis et al., 2021) after the introductions of a conceptual Autonomous Emergency Braking (AEB) system. The Near-Side, Far-Side, and Frontal impact originate from clusters #1, #2, and #4 accounting for 10.2%, 10% and 6% of the predicted crashes when either or both vehicles were equipped with the AEB system. For the Near-Side and Far-Side impacts, the highest opponent speed was selected as the impact speed and for the Frontal impact, the highest host speed was chosen.

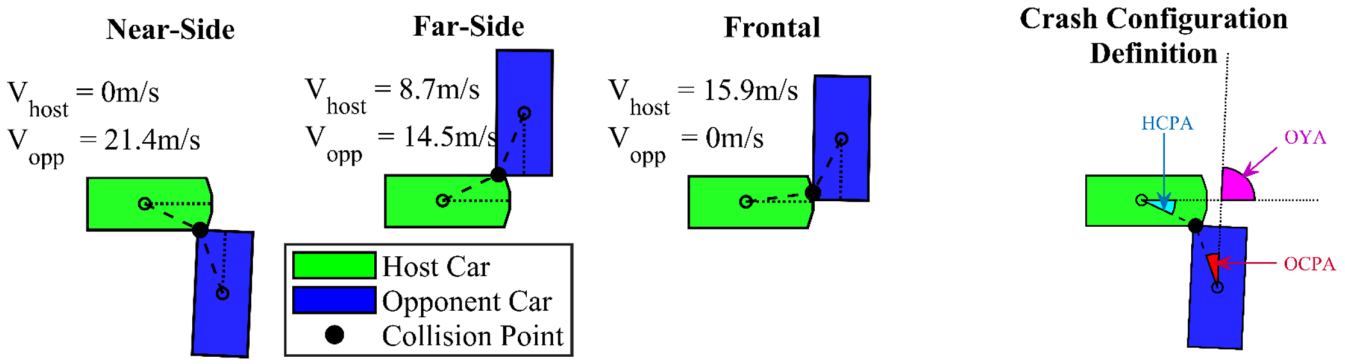

Fig C.1 The selected crash configurations. The impact velocity is visible for both vehicles in the figure. On the right, the Host Collision Point Angle (HCPA), Opponent Collision Point Angle (OCPA), and Opponent Yaw Angle (OYA) are visualized.

The in-crash motion of the vehicles is depicted in Fig C.2, and crash configuration and severity measures for the host vehicle are summarized in Table C.1.

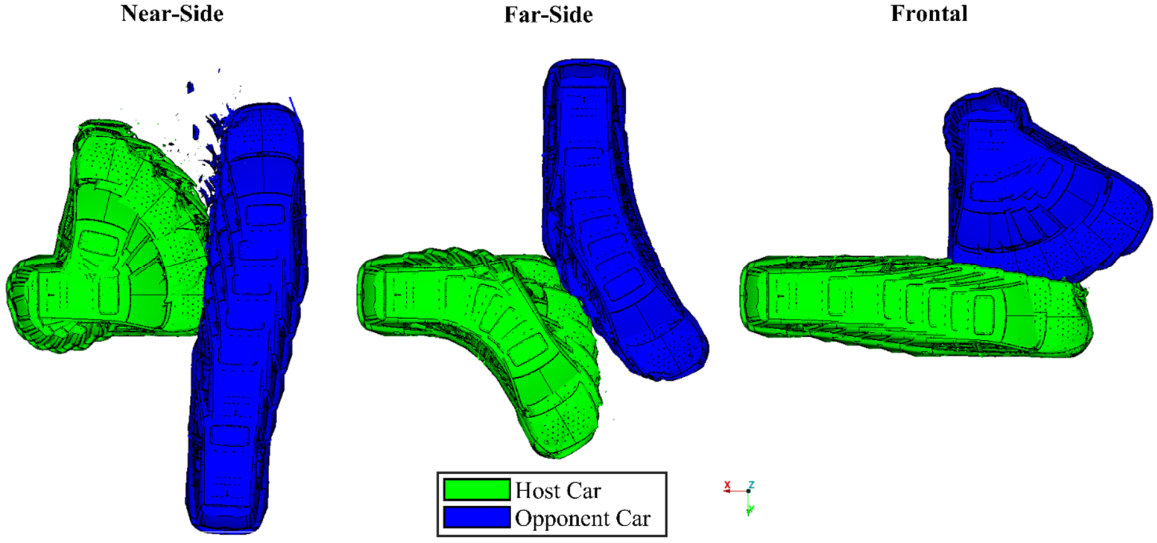

Fig C.2 Vehicle motion of car-car impact simulations. The host vehicle motion was used for the occupant in-crash simulations.

Table C.1 Crash Configurations and severity metrics according to Leledakis et al. (2021).

		Near-Side	Far-Side	Frontal
Crash Configuration	Host Collision Point Angle [°]	-48.3°	48.1°	17.5°
	Opponent Collision Point Angle [°]	42.4°	-42.7°	-48.4°
	Opponent Yaw Angle [°]	87.4°	-90.3°	-90.9°
	Host speed [m/s]	0	8.7	15.9
	Opponent speed [m/s]	21.4	14.5	0
Crash severity	ΔV resultant [m/s]	7.9	1.7	5.8
	Peak x-acc. [g]	11.8	5.1	22.7
	Peak y-acc. [g]	-18	26.8	7
	Peak resultant acc. [g]	21.3	26.9	22.9
	Peak z-rot. velocity [rad/s]	5.8	-4.4	0.7

Appendix D. Occupant Postures

A summary of the Occupant Sitting Postures (OSPs), which were constructed by combining body-region postures, can be seen in Appendix D. Table D.1 contains all OSPs. In sections D1-D4, OSPs containing variations of the lower extremity, torso, upper extremity, and head body region postures, respectively, can be seen.

Table D.1 Occupant Sitting Postures

OSP #	Seat-back angle	Lower Extremities	Torso		Upper Extremities	Head
			Sagittal Plane	Coronal Plane		
1	25° degrees	Right knee flexed	Nominal	Nominal	Over Knees	Nominal
2	25° degrees	Locked Ankles Right-Over	Nominal	Nominal	Over Knees	Nominal
3	25° degrees	Crossed Legs Right-Over	Nominal	Nominal	Over Knees	Nominal
4	25° degrees	Flexed knees	Nominal	Nominal	Over Knees	Nominal
5	25° degrees	Left knee flexed	Nominal	Nominal	Over Knees	Nominal
6	25° degrees	Locked Ankles Left-Over	Nominal	Nominal	Over Knees	Nominal
7	25° degrees	Crossed Legs Left-Over	Nominal	Nominal	Over Knees	Nominal
8	25° degrees	Nominal	Nominal	Nominal	Over Knees	Nominal
9	25° degrees	Nominal	Nominal	Nominal	Arms Crossed	Nominal
10	25° degrees	Nominal	Nominal	Nominal	Using Smartphone	Nominal
11	25° degrees	Nominal	Nominal	Nominal	Support in Arm Rest (door)	Nominal
12	25° degrees	Nominal	Nominal	Nominal	Support in Center Console	Nominal
13	25° degrees	Nominal	Nominal	Nominal	Over Knees	Rotated Left (60°)
14	25° degrees	Nominal	Nominal	Nominal	Over Knees	Rotated Right (55°)
15	25° degrees	Nominal	Nominal	Nominal	Over Knees	Rotated Right (80°)
16	25° degrees	Nominal	Nominal	Leaning Left	Over Knees	Nominal
17	25° degrees	Nominal	Nominal	Leaning Left	Support in Centre Console	Nominal
18	25° degrees	Nominal	Nominal	Leaning Right	Over Knees	Nominal
19	25° degrees	Nominal	Nominal	Leaning Right	Support in Arm Rest (door)	Nominal
20	30° degrees	Nominal	Semi-reclined	Leaning Left	Over Knees	Nominal
21	30° degrees	Nominal	Semi-reclined	Leaning Left	Support in Centre Console	Nominal
22	30° degrees	Nominal	Semi-reclined	Nominal	Over Knees	Nominal
23	30° degrees	Nominal	Semi-reclined	Nominal	Arms Crossed	Nominal
24	30° degrees	Nominal	Semi-reclined	Nominal	Using Smartphone	Nominal
25	30° degrees	Nominal	Semi-reclined	Nominal	Support in Arm Rest (door)	Nominal
26	30° degrees	Nominal	Semi-reclined	Nominal	Support in Centre Console	Nominal
27	30° degrees	Nominal	Semi-reclined	Leaning Right	Over Knees	Nominal
28	30° degrees	Nominal	Semi-reclined	Leaning Right	Support in Arm Rest (door)	Nominal
29	25° degrees	Nominal	Forward-leaning	Leaning Left	Over Knees	Nominal
30	25° degrees	Nominal	Forward-leaning	Leaning Left	Support in Centre Console	Nominal
31	25° degrees	Nominal	Forward-leaning	Nominal	Over Knees	Nominal
32	25° degrees	Nominal	Forward-leaning	Nominal	Support in Arm Rest (door)	Nominal
33	25° degrees	Nominal	Forward-leaning	Nominal	Support in Centre Console	Nominal
34	25° degrees	Nominal	Forward-leaning	Leaning Right	Over Knees	Nominal
35	25° degrees	Nominal	Forward-leaning	Leaning Right	Support in Arm Rest (door)	Nominal

D1. Lower Extremities

Besides the extended knees, which was the nominal posture, 7 additional OSPs were generated with variations of the lower extremity posture. The top, isometric, front, and left view can be seen in Fig D.1a - Fig D.1d, respectively.

Table D.2 Occupant Sitting Postures with manipulated lower extremity postures

OSP #	Lower Extremities	Seat-back angle	Torso		Upper Extremities	Head
			Sagittal Plane	Coronal Plane		
1	Right knee flexed	25° degrees	Nominal	Nominal	Over Knees	Nominal
2	Locked Ankles Right-Over					
3	Crossed Legs Right-Over					
4	Flexed knees					
5	Left knee flexed					
6	Locked Ankles Left-Over					
7	Crossed Legs Left-Over					
8	Extended Knees (Nominal)					

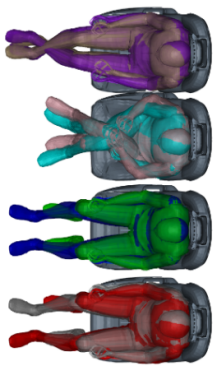

Fig D.1a Top View

Fig D.1b Isometric View

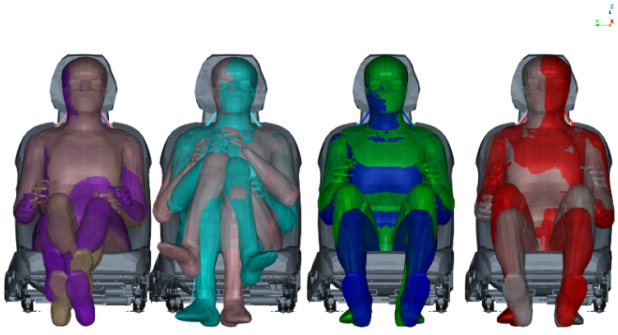

Fig D.1c Front View

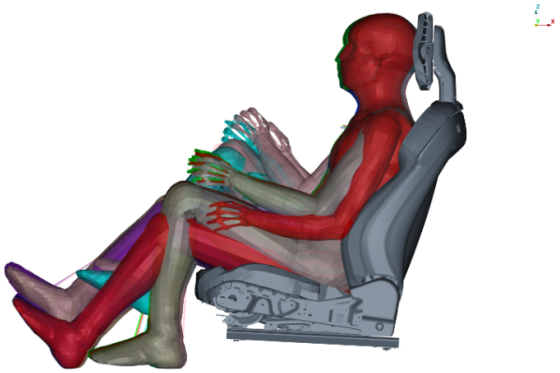

Fig D.1d Left View

D2. Torso

In the sagittal plane, the occupant was positioned in the nominal, semi-reclined and forward-leaning postures. Additionally, for every torso posture in the sagittal plane variations of the coronal posture were constructed with the occupant leaning left and right. The top, isometric, front, and left view can be seen in Fig D.2a - Fig D.2d, respectively.

Table D.3 Occupant Sitting Postures with manipulated torso postures

OSP #	Lower Extremities	Seat-back angle	Torso		Upper Extremities	Head
			Sagittal Plane	Coronal Plane		
8	Nominal	**25° degrees**	**Nominal**	**Nominal**	Over Knees	Nominal
16				Leaning Left		
18				Leaning Right		
22		30° degrees	Semi-reclined	Nominal		
20				Leaning Left		
27				Leaning Right		
31		25° degrees	Forward-leaning	Nominal		
29				Leaning Left		
34				Leaning Right		

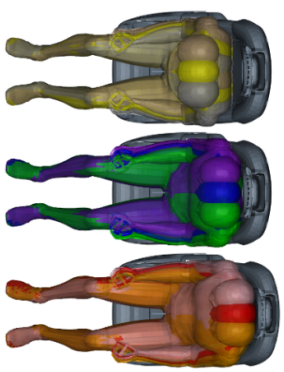

Fig D.2a Top View

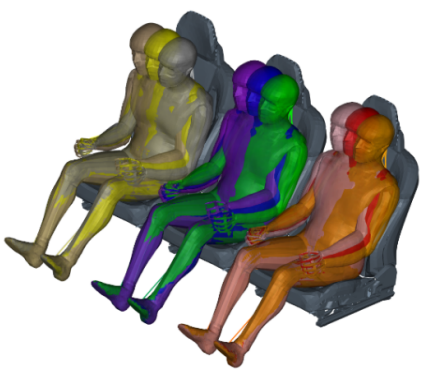

Fig D.2b Isometric View

Fig D.2c Front View

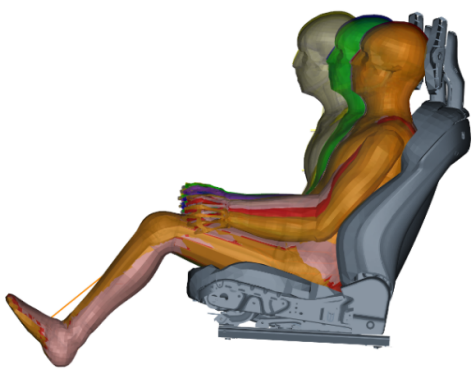

Fig D.2d Left View

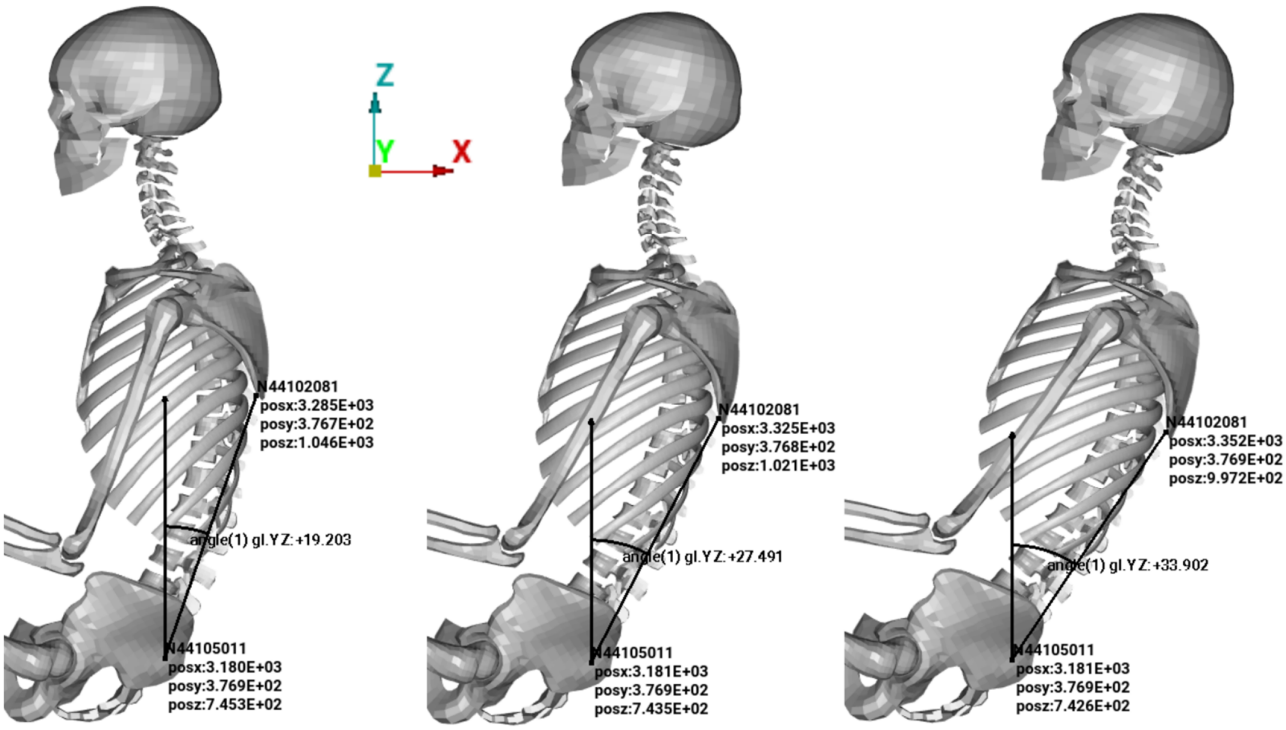

Fig D.2e Left View of the torso postures in the sagittal plane, with emphasis on the HBM skeleton

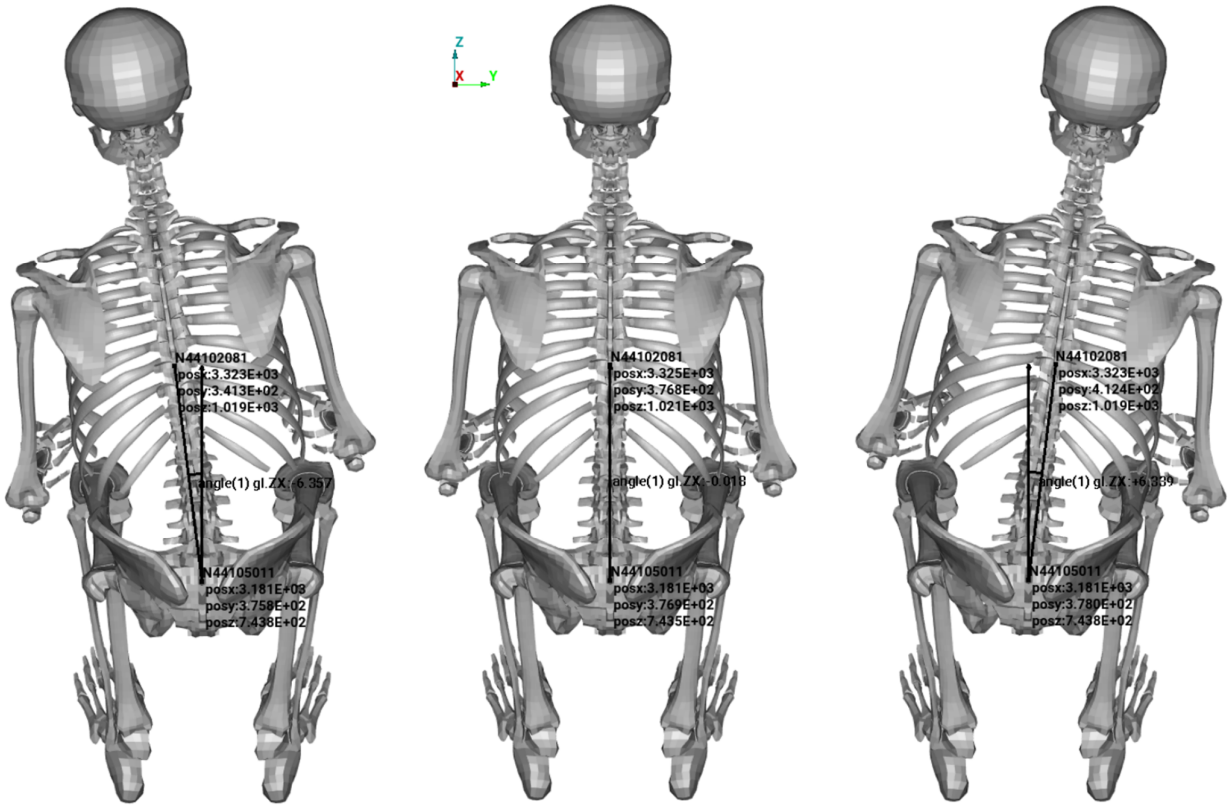

Fig D.2f Back View of the torso postures in the coronal plane, with emphasis on the HBM skeleton

D3. Upper Extremities

In total 25 OSPs with upper extremity posture variations were generated in 9 groups (one for every torso posture). The nominal upper extremity posture (with hands placed over the knees) of every group was used as the reference in the cross-correlation analysis.

Table D.4 Occupant Sitting Postures with manipulated upper extremity postures

OSP #	Lower Extremities	Seat-back angle	Torso		Upper Extremities	Head
			Sagittal Plane	Coronal Plane		
8	Nominal	25° degrees	Nominal	Nominal	**Over Knees**	Nominal
9					Arms Crossed	
10					Using Smartphone	
11					Support in Arm Rest (door)	
12					Support in Center Console	
16				Leaning Left	**Over Knees**	
17					Support in Center Console	
18				Leaning Right	**Over Knees**	
19					Using Smartphone	
22		30° degrees	Semi-reclined	Nominal	**Over Knees**	
23					Arms Crossed	
24					Using Smartphone	
25					Support in Arm Rest (door)	
26					Support in Center Console	
20				Leaning Left	**Over Knees**	
21					Support in Center Console	
27				Leaning Right	**Over Knees**	
28					Support in Arm Rest (door)	
31		25° degrees	Forward-leaning	Nominal	**Over Knees**	
32					Support in Arm Rest (door)	
33					Support in Center Console	
29				Leaning Left	**Over Knees**	
30					Support in Center Console	
34				Leaning Right	**Over Knees**	
35					Support in Arm Rest (door)	

Fig D.3a - Fig D.3d, include the top, isometric, front, and left view, respectively, in which variations of upper extremity postures when the occupant is sitting with the nominal torso posture can be seen. In Fig D.3e - Fig D.3f, the “Arms Crossed” and “Using Smartphone” postures can be seen in detail.

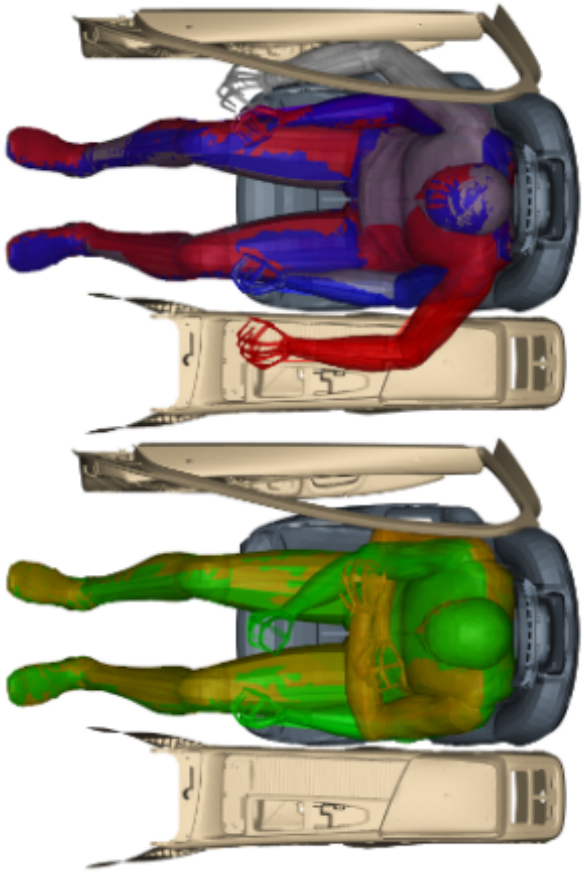

Fig D.3a Top View

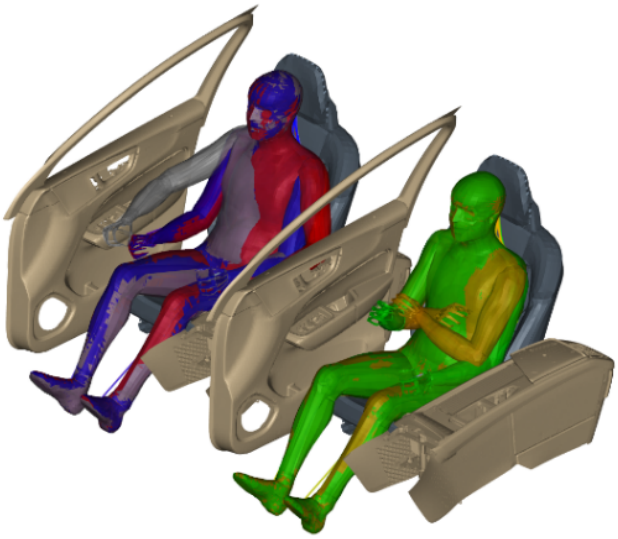

Fig D.3b Isometric View

Fig D.3c Front View

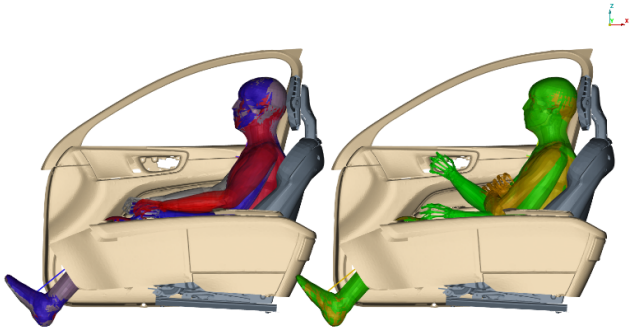

Fig D.3d Left View

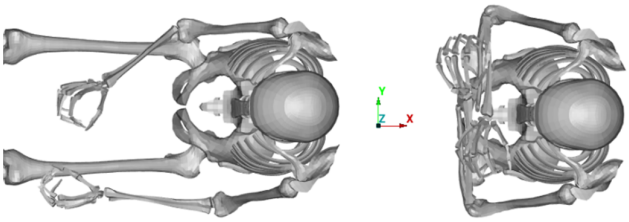

Fig D.3e Top View of the “Arms Crossed” and “Using Smartphone” postures

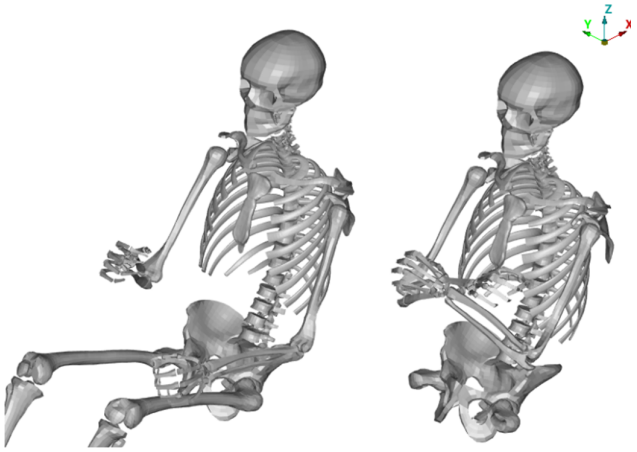

Fig D.3f Isometric View of the “Arms Crossed” and “Using Smartphone” postures

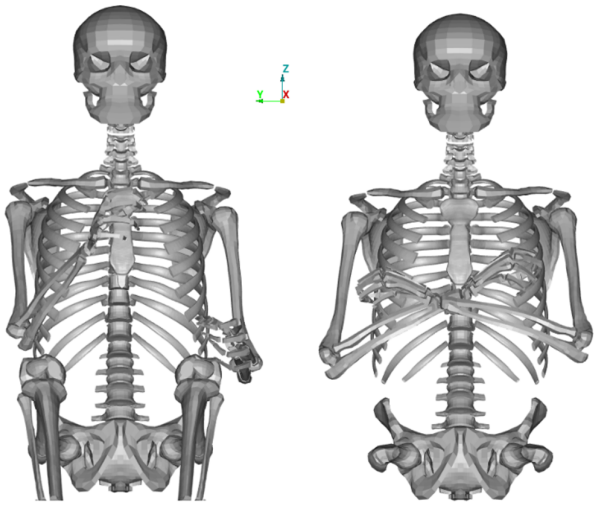

Fig D.3g Front View of the “Arms Crossed” and “Using Smartphone” postures

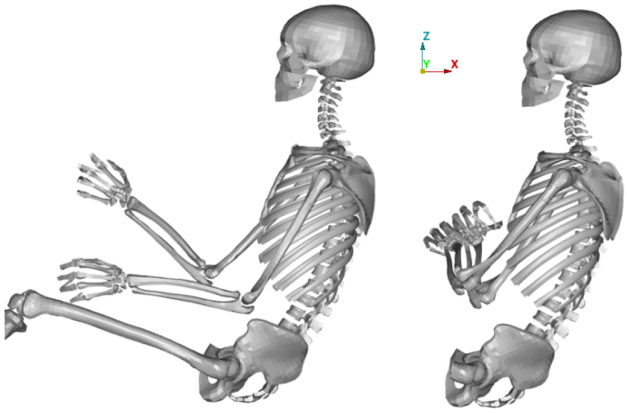

Fig D.3h Left View of the “Arms Crossed” and “Using Smartphone” postures

D4. Head

Head postures, adapted from Fice et al. (2018), were used to construct three additional OSPs. The top, isometric, front, and left view can be seen in Fig D.4a - Fig D.4d, respectively.

Table D.5 Occupant Sitting Postures with manipulated head postures

OSP #	Lower Extremities	Seat-back angle	Torso		Upper Extremities	Head			
			Sagittal Plane	Coronal Plane		Orientation	Yaw	Pitch	Roll
8	Nominal	25° degrees	Nominal	Nominal	Nominal	Nominal	-0.4°	0°	0.6°
13						Rotated Left (60°)	59.3°	-3.7°	3.7°
14						Rotated Right (55°)	-54.6°	-11.3°	0.4°
15						Rotated Right (80°)	-80.6°	-8.1°	2°

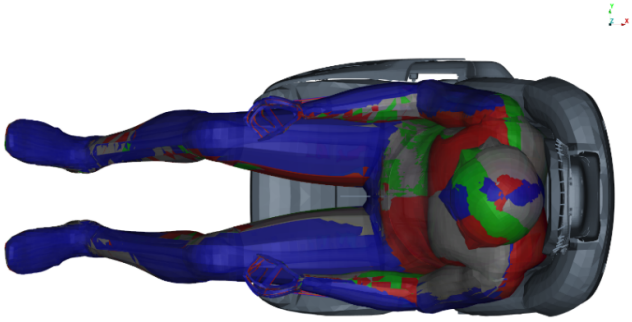

Fig D.4a Top View

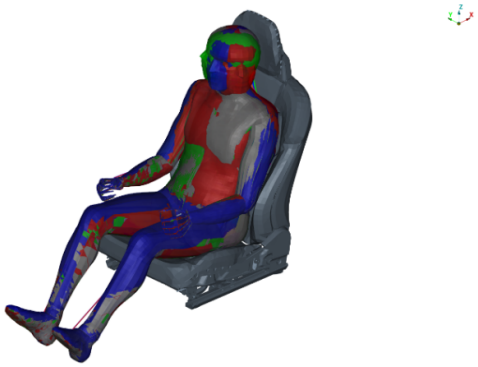

Fig D.4b Isometric View

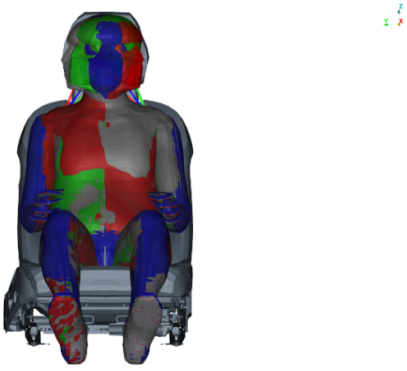

Fig D.4c Front View

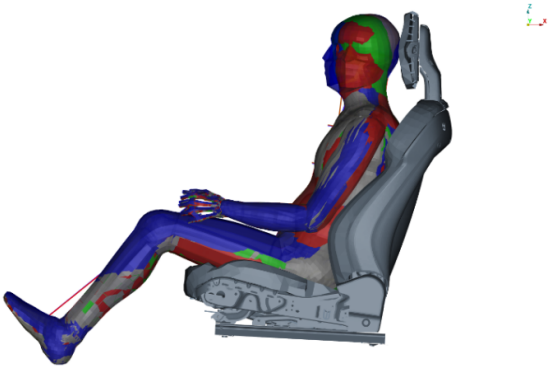

Fig D.4d Left View

Appendix E. Belt Fit

E1. Lower Extremities

Only minor variations were seen in belt fit, with the exception of the crossed legs posture.

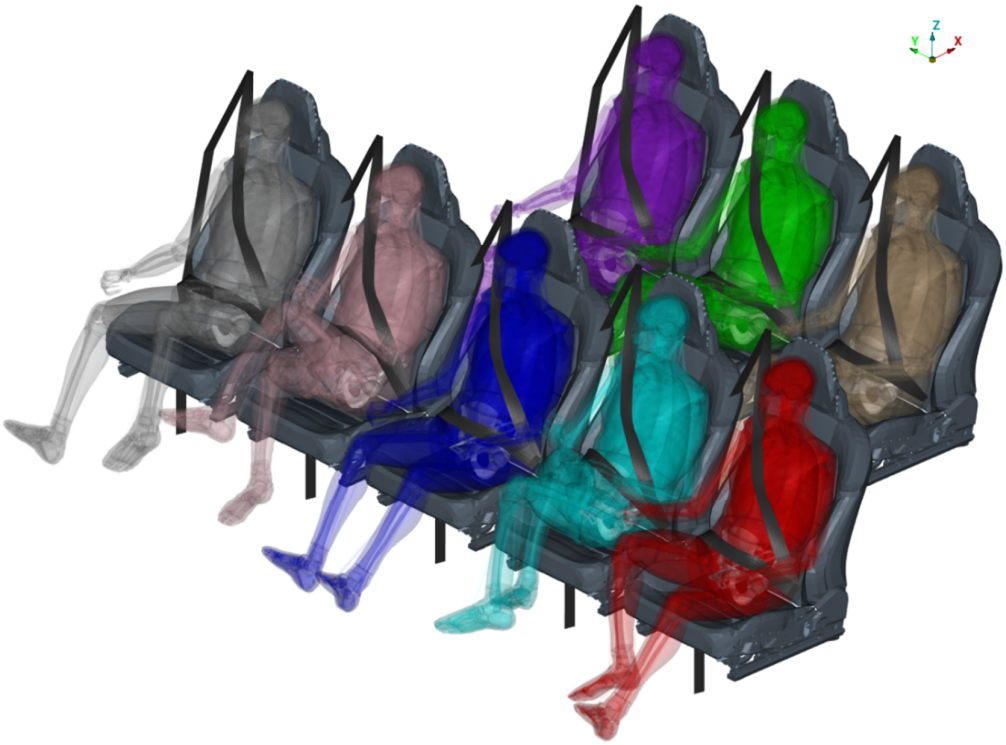

Fig E.1a Isometric view of the lower extremity postures with focus on belt fit.

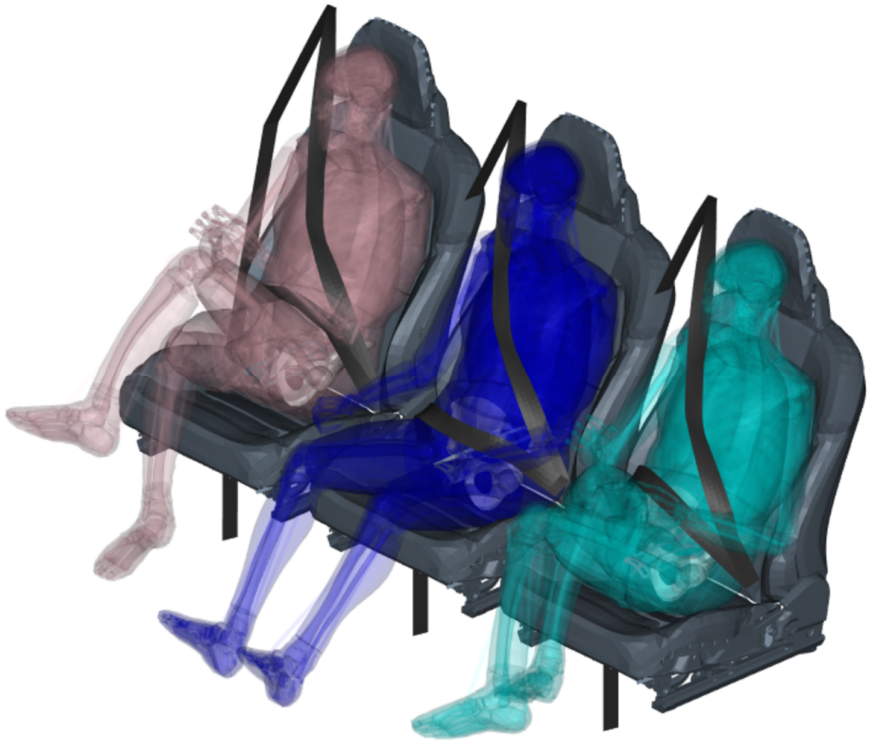

Crossed Legs Left-Over Crossed Legs Right-Over Extended Knees (Nominal)

Fig E.1b Isometric view of the lower extremity postures with focus on belt fit. The nominal and the crossed legs postures can be seen

The lap belt - buckle side (inboard) - is placed higher on the pelvis (left ASIS) when the legs are crossed. This is more visible when the left leg is crossed over the right knee (Fig E.1c). The lap belt - anchor side (outboard) - is placed higher on the pelvis (right ASIS) when the legs are crossed (Fig E.1d). This is more visible when the right leg is crossed over the left knee. In all postures, the lap belt is below the left and right ASIS.

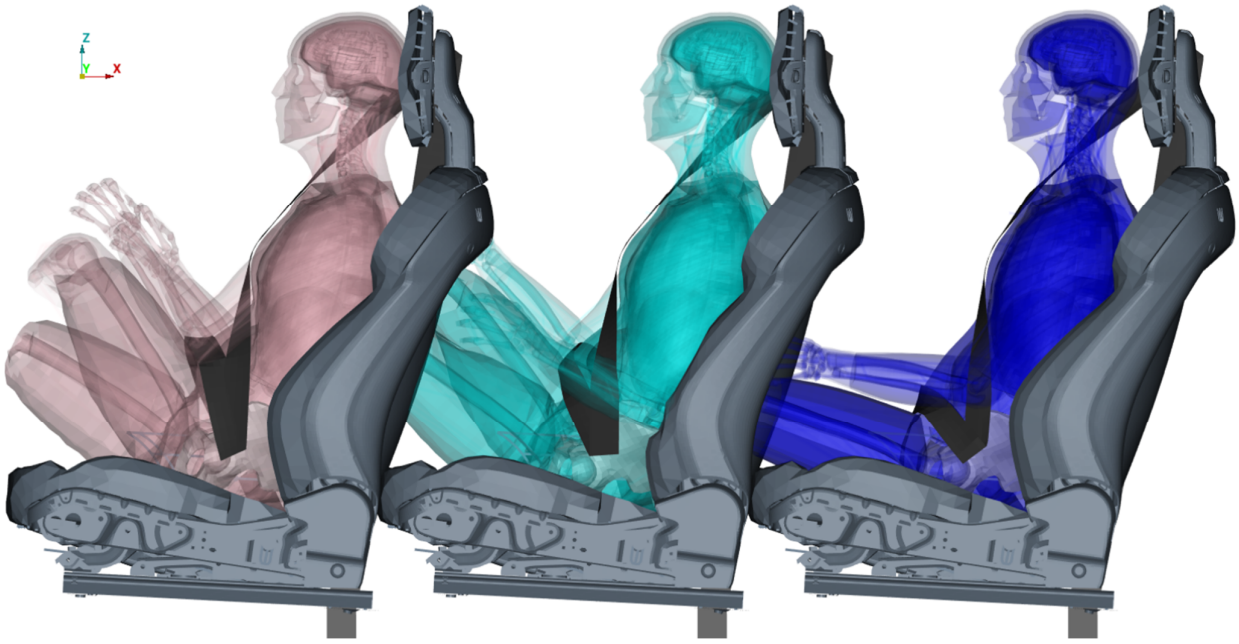

Crossed Legs Left-Over | Crossed Legs Right-Over | Extended Knees (Nominal)

Fig E.1c Left view of the lower extremity postures with focus on the lap belt fit. The crossed legs (left-over and right-over) postures can be seen next to the nominal posture.

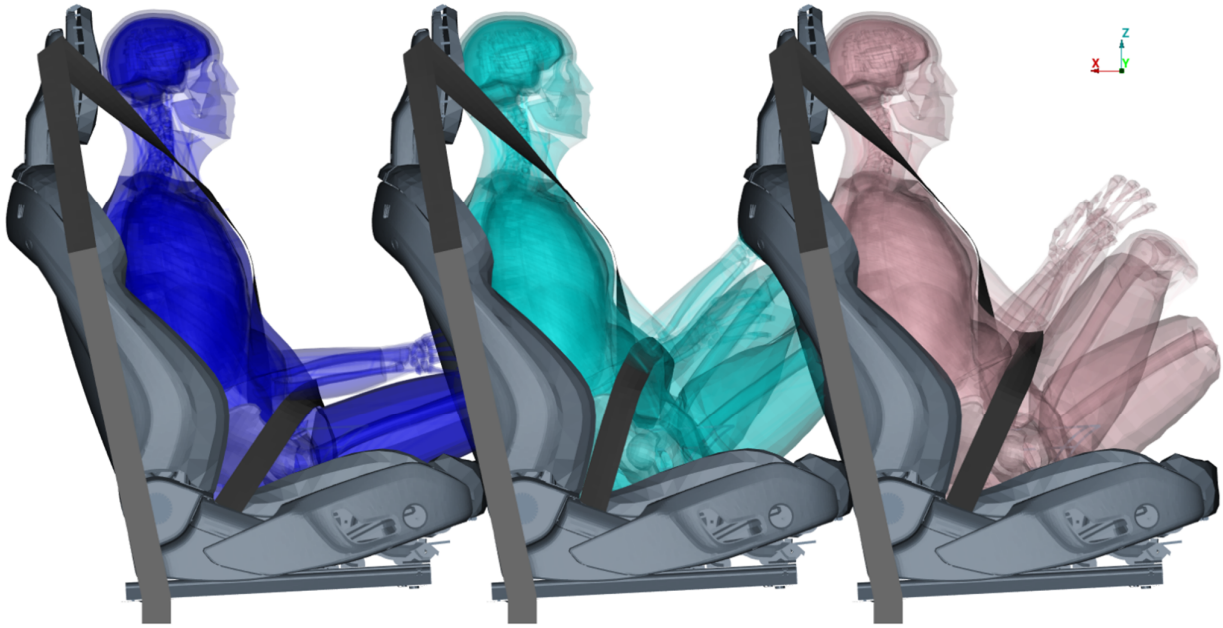

Extended Knees (Nominal) | Crossed Legs Right-Over | Crossed Legs Left-Over

Fig E.1d Right view of the lower extremity postures with focus on the lap belt fit. The crossed legs (left-over and right-over) are seen next to the nominal posture.

E2. Torso

The main variations can be seen in the shoulder belt fit when the posture is changed in the coronal plane.

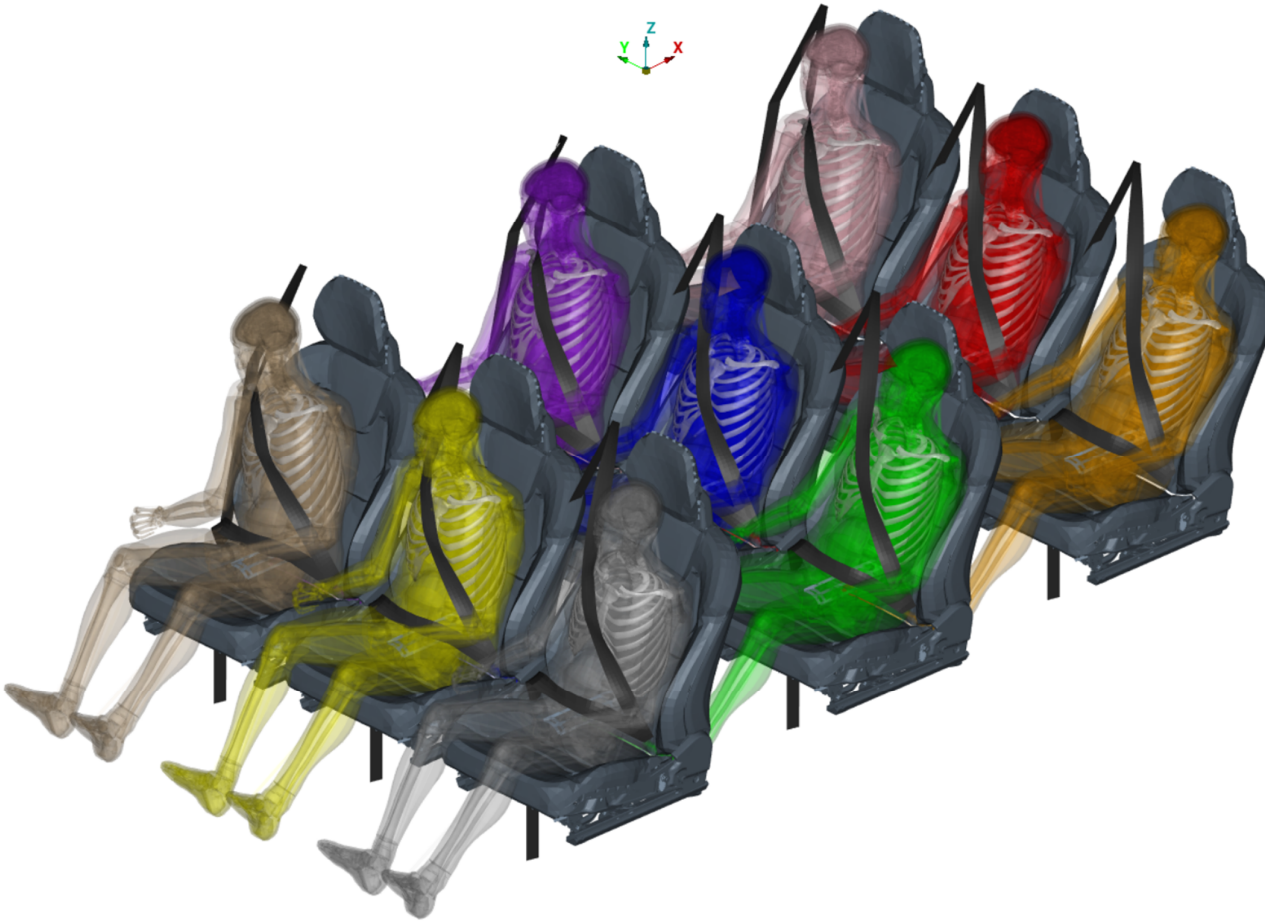

Fig E.2a Isometric view of the torso postures with focus on belt fit.

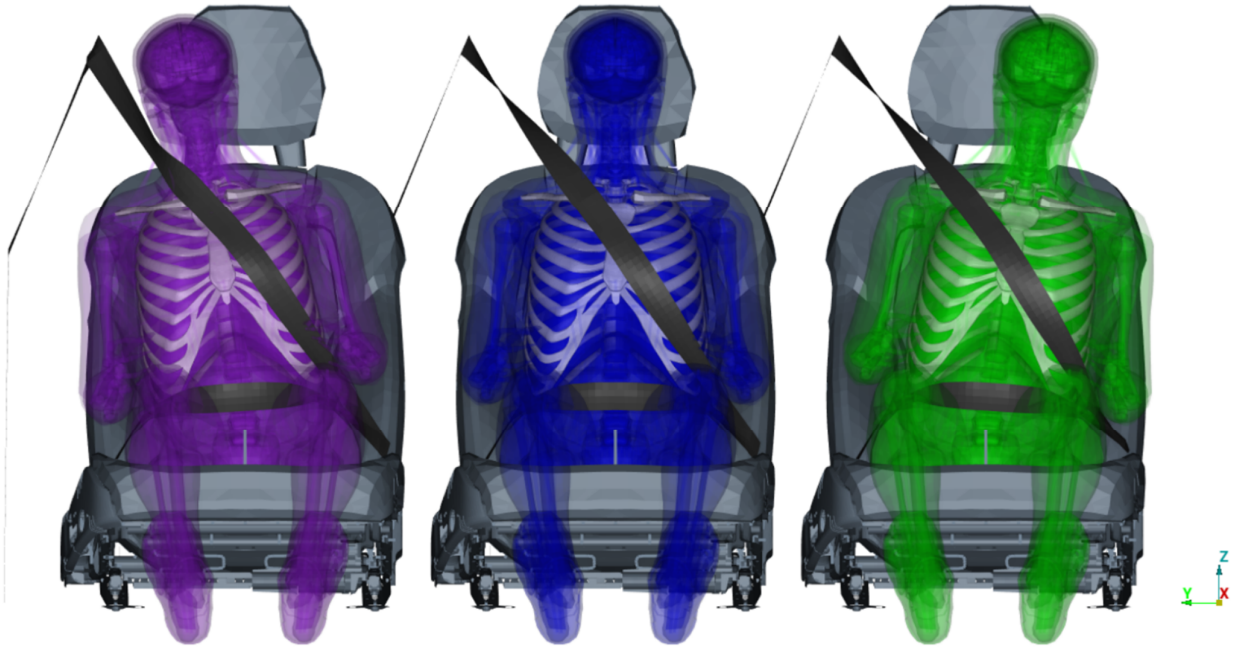

Leaning left Nominal Leaning Right

Fig E.2b Front view of the torso coronal postures with focus on the shoulder belt fit.

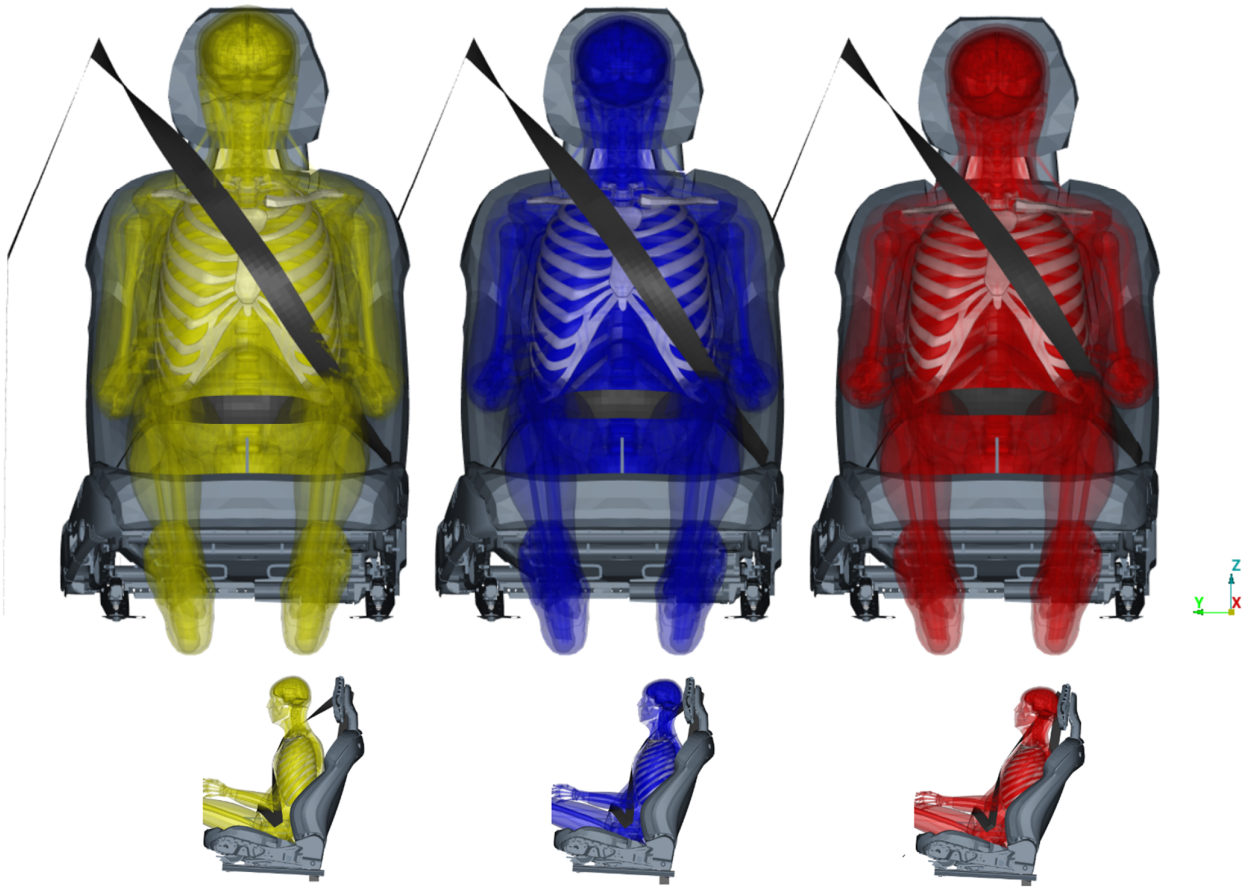

Forward-leaning Nominal Semi-reclined

Fig E.2c Front view of the torso sagittal postures with focus on the shoulder belt fit.

Appendix F. Occupant Responses

The landmarks used for the kinematic and kinetic analysis, as described in section 2.5 and summarized in Table 1 (see main body of the publication) and can be seen in **Error! Reference source not found.**Appendix F.

F1. Lower Extremities

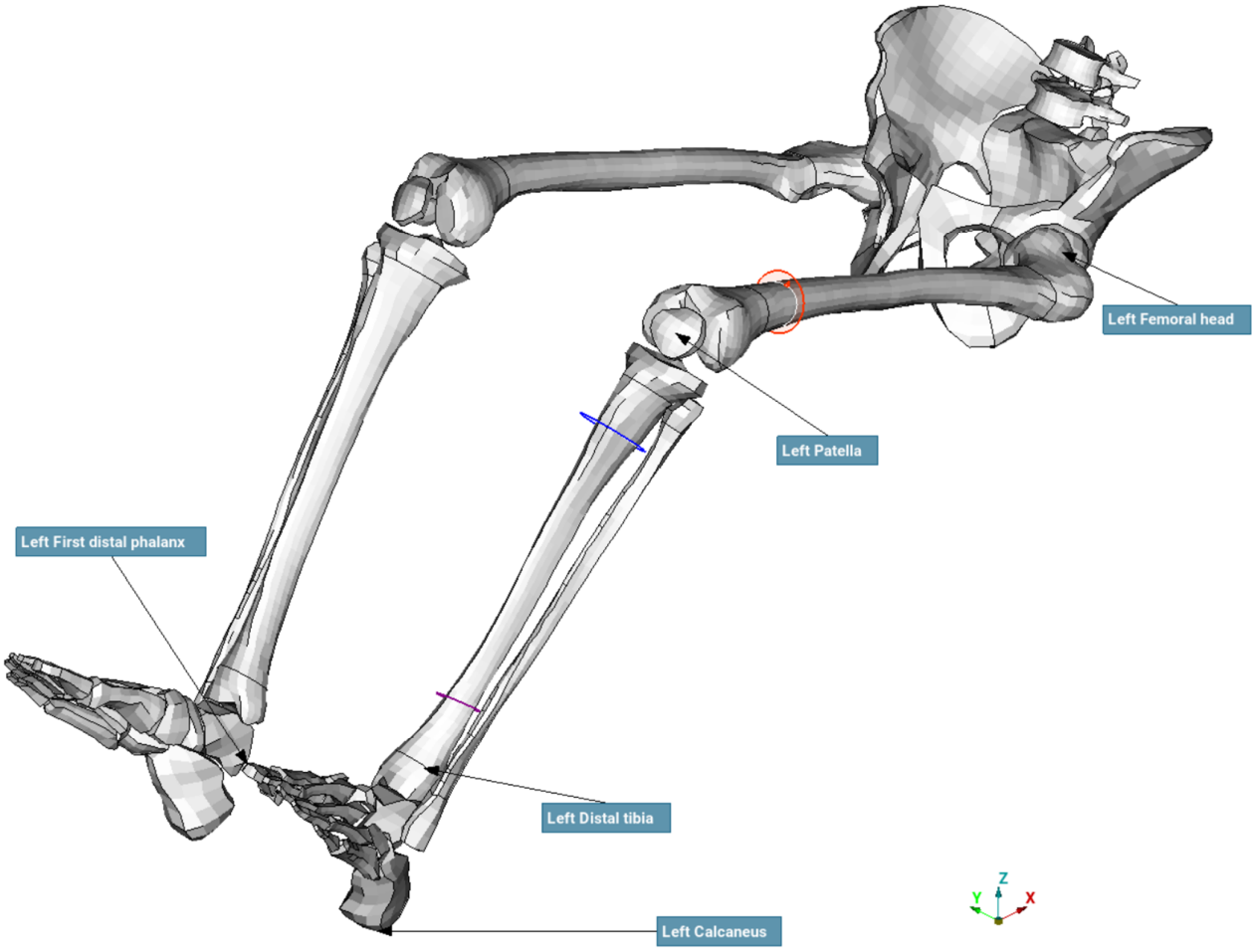

Fig F.1 Isometric view with the landmarks and cross-sections of the left lower extremity. The distal femur (red), proximal tibia (blue), and distal tibia (purple) cross-sections can be seen.

F2. Pelvis

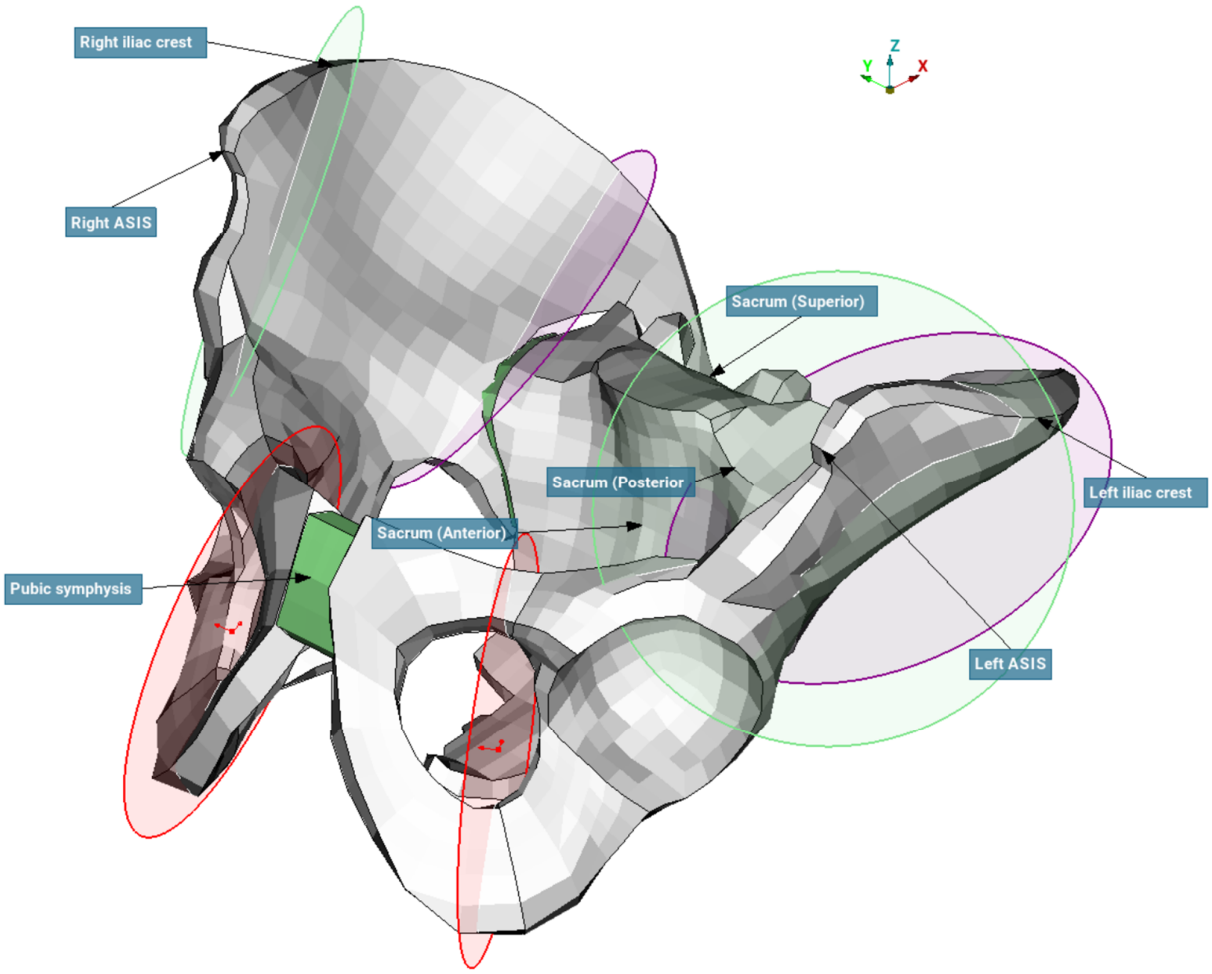

Fig F.2a Isometric view with the landmarks and cross-sections of the pelvis. The pubic rami (red), SI joint (purple), and ASIS (green) cross-sections can be seen.

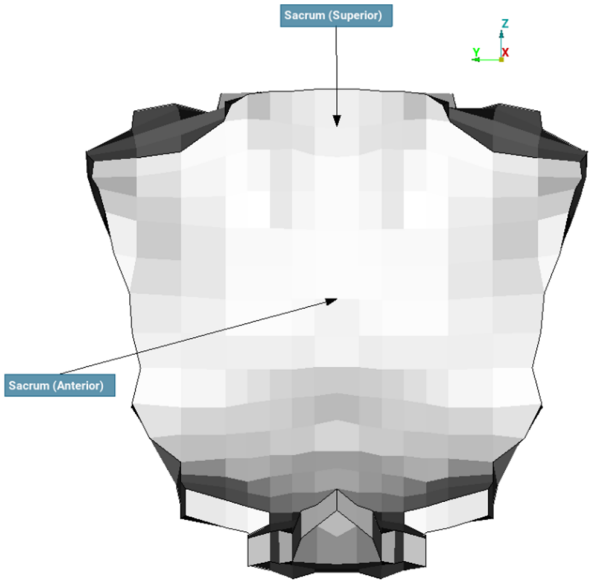

Fig F.2b Front view of the sacrum. The anterior sacrum landmark selected is visible.

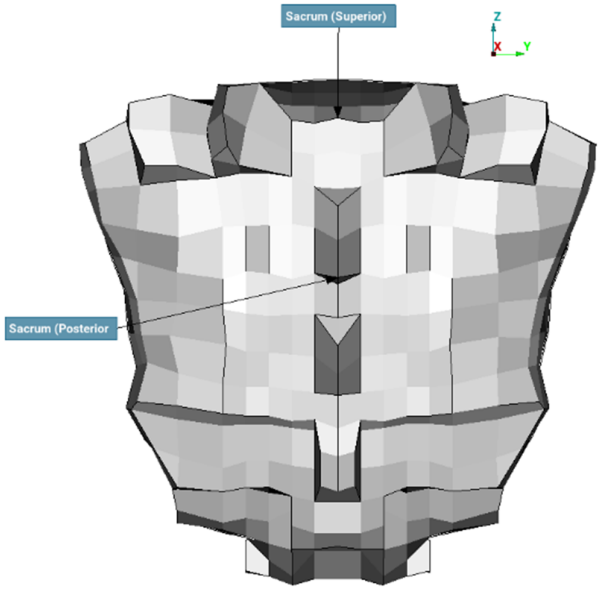

Fig F.2c Rear view of the sacrum. The posterior sacrum landmark selected is visible.

F3. Torso

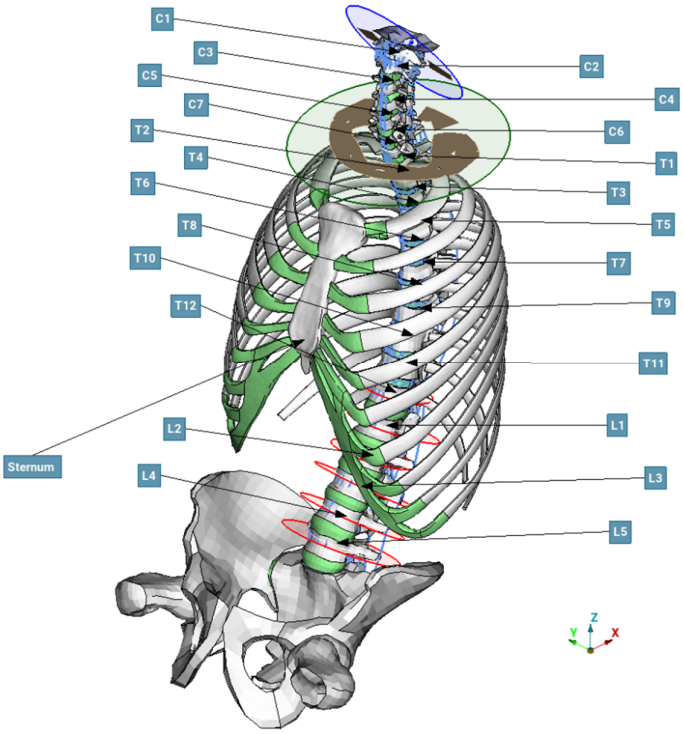

Fig F.3a Isometric view of the torso, spine and pelvis. The upper neck (blue), lower neck (green), and T12-L5 (red) cross-sections can be seen.

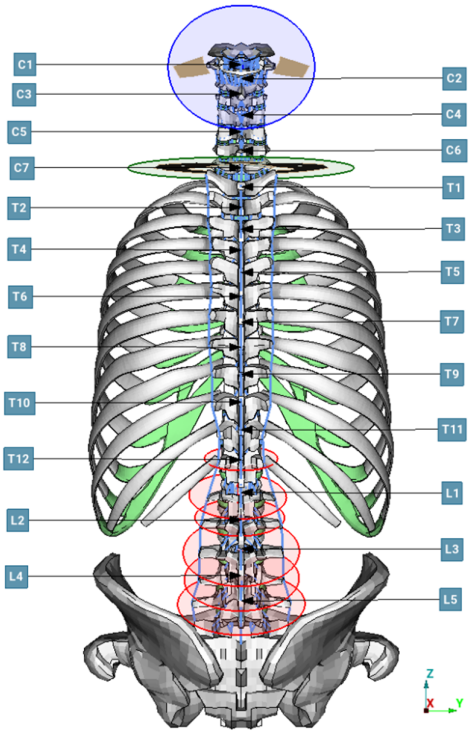

Fig F.3b Rear view of the torso, spine and pelvis.

F4. Upper Extremities

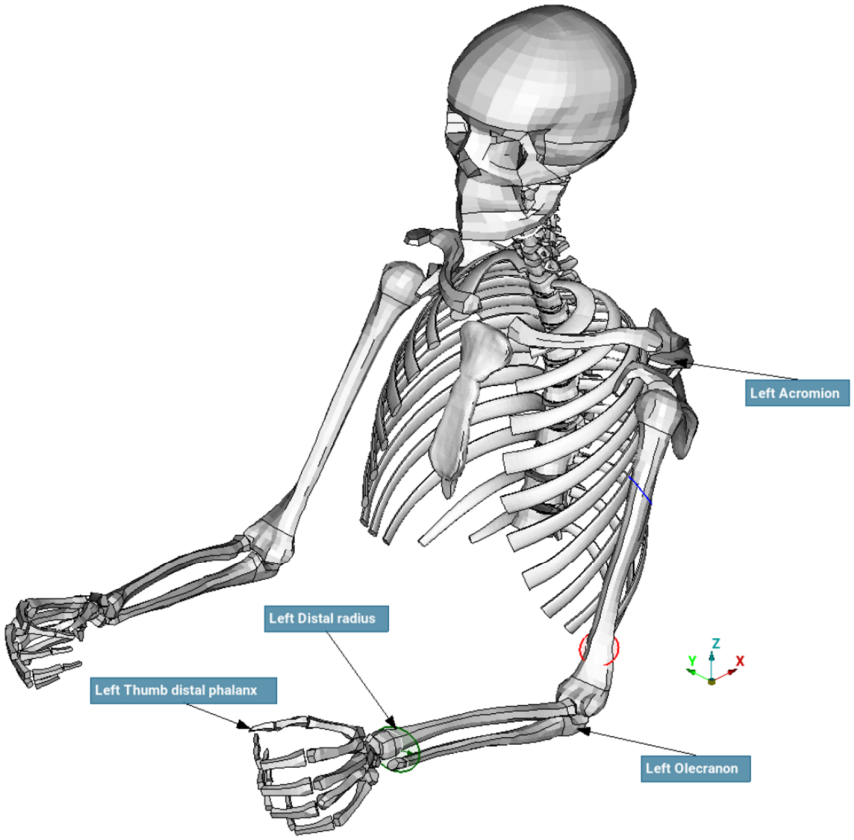

Fig F.4 Isometric view with the landmarks and cross-sections of the left upper extremity. The proximal humerus (blue), distal humerus (red), and distal forearm (green) cross-sections can be seen.

F5. Head

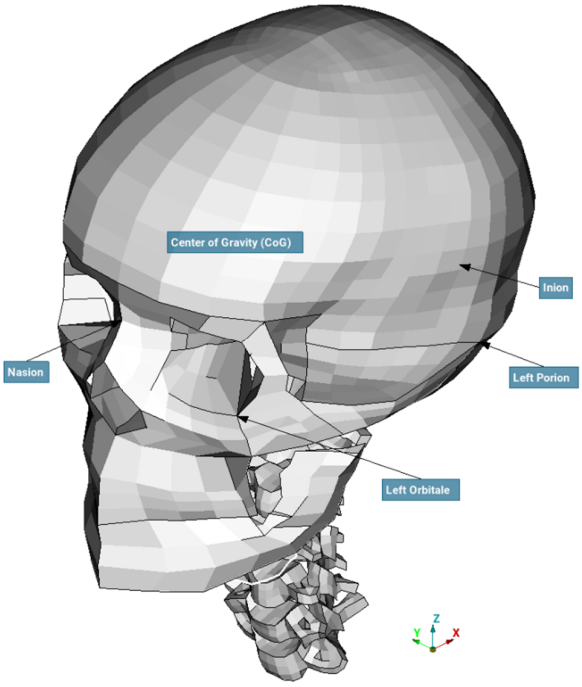

Fig F.5a Isometric view of the head.

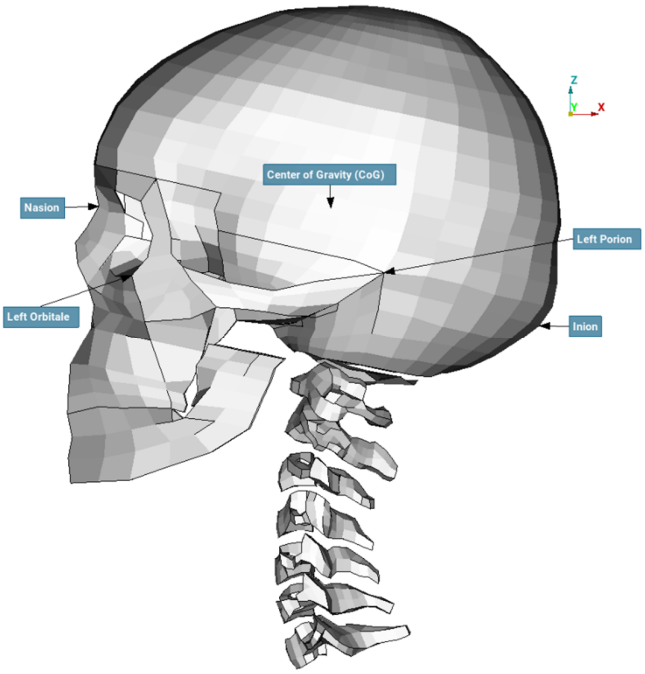

Fig F.5b Left view of the head.